AN EXPERIMENTAL INVESTIGATION OF THE SENSITIVITY OF A BURIED FIBER OPTIC INTRUSION SENSOR

A Thesis

by

HARINI KUPPUSWAMY

Submitted to the Office of Graduate Studies of
Texas A&M University
in partial fulfillment of the requirements for the degree of

MASTER OF SCIENCE

December 2005

Major Subject: Electrical Engineering

AN EXPERIMENTAL INVESTIGATION OF THE SENSITIVITY OF A BURIED FIBER OPTIC INTRUSION SENSOR

A Thesis

by

HARINI KUPPUSWAMY

Submitted to the Office of Graduate Studies of
Texas A&M University
in partial fulfillment of the requirements for the degree of

MASTER OF SCIENCE

Approved by:

Chair of Committee,	Henry F. Taylor
Committee Members,	Chin B. Su
	Narasimha Reddy
	Lihong Wang
Head of Department,	Costas Georghiades

December 2005

Major Subject: Electrical Engineering

ABSTRACT

An Experimental Investigation of the Sensitivity of
a Buried Fiber Optic Intrusion Sensor. (December 2005)
Harini Kuppuswamy, B.Eng., University of Poona, India
Chair of Advisory Committee: Dr. Henry F. Taylor

A distributed fiber optic sensor with the ability of detecting and locating intruders on foot and vehicles over long perimeters (>10 km) was studied. The response of the sensor to people walking over or near it and to vehicles driving nearby was observed and analyzed. The sensor works on the principle of phase sensitive optical time domain reflectometry, making use of interferometric effects of Rayleigh backscattered light along a single mode fiber. Light pulses from a highly stable Er:doped fiber laser emitting single longitudinal mode light and exhibiting low frequency drift are passed through one end of the buried fiber. The backscattered light emerging from the same fiber end was monitored using a photodetector. The phase changes produced in the light pulse due to the pressure of the intruder walking directly above or near the sensor or from the seismic disturbances created by vehicles moving in the vicinity of the sensor are detected using the phase sensitive Optical Time Domain Reflectometer (ϕ-OTDR).

Field tests were conducted with the sensing element as a single mode fiber in a 3-mm diameter cable buried at depths ranging from 8 to 18 inches in clay soil. It was observed that the sensor could detect intruders walking transverse to the cable line at a distance of 40 ft from it. A car moving at a speed of 30 mph on a rough road could be consistently detected up to a distance of 480 ft from the sensor, while a car driven on a smooth road 200 ft from the sensor could be detected only when passing through rough patches on the road. Tests were also performed with an intruder walking near

the sensor while a car was driven at a speed of 30 mph on a rough road. The effect on the signal due to the intruder on foot could be distinguished clearly only when the car was at least 200 ft away from the sensor.

The results in this thesis represent the first quantitative study of the sensitivity of the sensor under varied test conditions. It is expected that these findings will be helpful in the practical implementation of the long perimeter intrusion sensor along high security domains like national borders, military bases and government buildings.

To My Greatest Strength: My Parents, Sister and Husband

ACKNOWLEDGMENTS

I would like to express my sincere gratitude and thanks to Dr. Henry F. Taylor, the chairman of my advisory committee, for his guidance and counsel throughout my research process. I will always hold him in high esteem for the understanding, patience and support he showed me during all times. I would also like to express my appreciation to Dr. Chin B. Su, Dr. Narasimha Reddy and Dr. Lihong Wang for volunteering their time to serve on my graduate committee. My appreciation to Juan C. Juarez for his guidance and help throughout my research. Special thanks go to Bilal Malik, Myung J. Lee, Shankarram Subramanian and Rajesh Pasupathi for their helpful discussions, aid and support.

My deepest gratitude goes to my family for their constant support, encouragement and for being always there for me. Finally, I would like to thank God for making this possible for me.

TABLE OF CONTENTS

Page

LIST OF FIGURES

FIGURE Page

FIGURE Page

FIGURE Page

CHAPTER I

INTRODUCTION

In today's world, security in private and public sectors has become an issue of great importance for all the countries worldwide. All nations are interested in developing and transitioning capabilities that improve the security of the national border without impedance to the flow of commerce and travelers. The United States of America has 7,000 miles of international land border with Canada and Mexico which has 20 sectors responsible for detecting, interdicting and apprehending those who attempt to illegally enter or smuggle people, including terrorists, or contraband, including weapons of mass destruction, across U.S. borders between official ports of entry. The number of illegal crossings along Arizona's 200 miles of border with Mexico alone was 1.5 million in the year 2003 [1]. Thus, for surveillance of the borders, sensor detection range is a major factor. The long perimeter fiber optic sensor discussed in this thesis is a good candidate for a long range covert intrusion detection system.

Today's perimeter security systems use a variety of techniques including seismic, acoustic, magnetic and infrared sensors for monitoring the domain of interest. A limitation with these methods is that they require the wireless transmission of data [2]. Also, these sensors have lower range of detection and may not show multiple intrusions at the same time. Fiber optic sensors have created their own niche because of their small size, lower weight, lower power consumption, resistance to electromagnetic interference, higher sensitivity, wider bandwidth, lower cost and ruggedness [3]. The fiber optic sensors are also hidden and passive.

Disturbances can be produced in an optical fiber due to geometrical or optical

---

The journal model is *IEEE Transactions on Automatic Control.*

changes. These disturbances are minimized in fiber optic communication systems to reduce noise in the transmitted signal. However, in fiber optic sensors the effect of a particular disturbance of interest is emphasized. Due to the revolutionary changes in the field of fiber optics and optoelectronic devices over the past twenty years, there has been a great improvement in the fiber optic sensor technology. The advances made in the fiber optic communications and photonics industry over this period have led to mass production of opto-electronic components and fiber optic cables thereby providing low cost components for use in the sensors.

The preliminary fiber optic sensor for detection of intruders was initially proposed over a decade ago [4]. The sensor was configured as a Optical Time Domain Reflectometer (OTDR) with a highly coherent laser as the light source. The conventional OTDR can detect the presence and location of the perturbation but it does not detect phase changes in the backscattered light. The system has been modified over the years to yield a more practical intruder sensor with higher sensitivity and reliability. This sensor uses a phase sensitive Optical Time Domain Reflectometer (ϕ-OTDR) instead of the conventional OTDR. In the present system, the phase change produced in the backscattered light due to the pressure of the intruder on the ground is observed using a ϕ-OTDR. Thus, the ϕ-OTDR is sensitive to perturbations which are too small to be detected by the conventional OTDR. In comparison with the conventional OTDR the ϕ-OTDR requires a laser source with very low frequency drift as well as very narrow linewidth to achieve the necessary phase sensitivity. For meeting the necessary criteria a very highly stable Er-doped fiber laser is used [5]. In this sensor, the fiber can be connected to all the signal processing electronics located centrally in a protected site, with the distributed fiber sensor extending a distance 10 km or more away from the actual location of detection.

This thesis research represents the first quantitative study of the sensor response

under various test conditions. Experiments were carried out in the field with intruders on foot and moving vehicles to characterize the sensor. Tests were also conducted to study the response of the sensor when an intruder and a moving vehicle were simultaneously present. The drop in sensor response as a function of lateral distance from the buried cable for both people on foot and vehicles is also characterized. Thus, a quantitative indication of the lateral range of the sensor for both intruders on foot and motor vehicles is presented in the thesis. This thesis presents the theoretical background of the sensor, experimental procedures used for the quantitative analysis, results, conclusions and recommendations for future work.

CHAPTER II

BACKGROUND

A. Optical Fibers

The transmission of light through a dielectric waveguide structure was first proposed and investigated at the beginning of the twentieth century. This proved to be an impractical one due to its unsupported structure. However, interest in the field led to the development of a clad dielectric waveguide. This problem was overcome by the optical fiber having a cladding with over the core with refractive index slightly lower than the core. Depending upon certain dimensions of the core and cladding the fiber can be single mode or multi mode. In this thesis we are using a single mode fiber as the light is characterized by a single phase value. Although single mode fibers have small core diameters, the cladding diameter must be at least ten times the core diameter to avoid losses from the evanescent field. The core is usually very pure glass like fused silica (SiO_2) doped with germania (GeO_2). The core is surrounded by the cladding, generally pure fused silica, having slightly lesser refractive index than the core. The primary fiber is given a buffer coating to protect the fiber from external mechanical and environmental influences like microbending. The buffer having highest refractive index absorbs the light propagating in the cladding in a very short distance [6]. An optical fiber structure looks as shown in Fig. 1.

In an optical fiber an injected pulse of light can travel through tens of kilometers of fiber. The propagation of light through an optical fiber can be explained by the principle of Total Internal Reflection (TIR). The acceptance angle for a fiber, θ_a is the angle of incidence between the incident light ray and fiber axis, is given by eq. 2.1

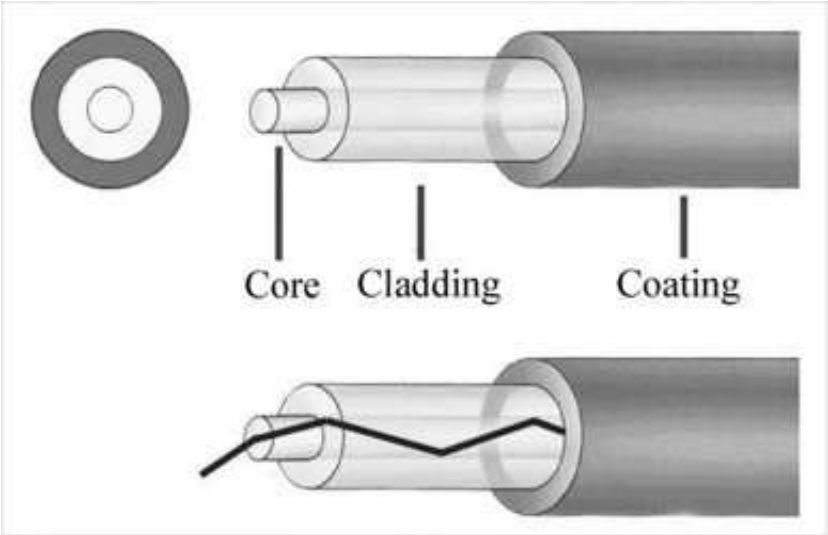

Fig. 1. Structure of an optical fiber

$$\sin\theta_a = \sqrt{n_1^2 - n_2^2} \tag{2.1}$$

The refractive index n_1 is that of the core and n_2 indicates the refractive index of the cladding. Only rays emitted within a cone having a full angle $2\theta_a$ will be trapped and propagated through the fiber as shown in Fig. 2.

There are three transmission windows in an optical fiber. The first transmission window range is between 800 nm - 900 nm. The second transmission window is between 1300 nm - 1600 nm and the third window is centered around 1550 nm which has the minimum attenuation. The Er:doped laser used in these experiments operates at 1555.4 nm in the third window due to its compatibility with the Er:doped Fiber Amplifiers [7]. The transmission windows are as shown in Fig. 3 [8].

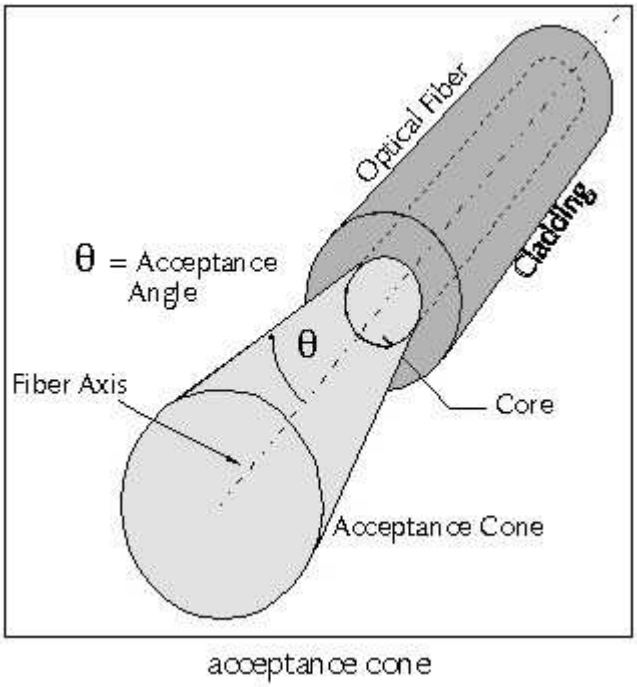

Fig. 2. Propagation of light wave through an optical fiber

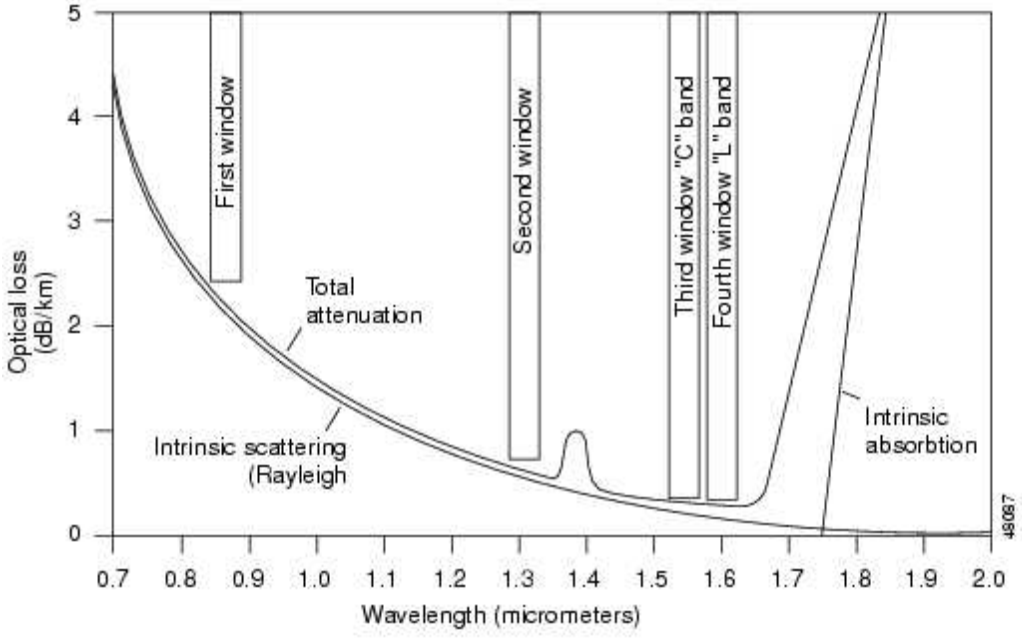

Fig. 3. Attenuation of optical fiber showing major wavelength regions

B. Rayleigh Scattering in a Single Mode Fiber

Rayleigh scattering is the dominant intrinsic loss in the transmission window between the ultraviolet and infrared absorption tails. It results from inhomogeneities of a random nature occurring on a small scale compared to the wavelength of the light. These inhomogeneities are produced from the variations of density and composition which are frozen into the glass during the drawing of the fiber. These variations result in refractive index fluctuations that may be modeled as small scattering centers embedded in an otherwise homogeneous material [7].

As a beam of light travels through an optical fiber, some of its energy will be scattered in all directions by these scattering centers. This is illustrated in Fig. 4. A small part of this scattered light will be recaptured by fiber core and guided toward the source. The measurement and analysis of the Rayleigh backscattered light is used in Optical Time Domain Reflectometry (OTDR). The OTDR provides measurement of the attenuation on an optical fiber along its entire length, giving information on the length dependence of the loss. The Rayleigh scattering loss produces an attenuation proportional to λ^{-4} throughout the visible and near-infrared spectral regions with a minimum of 0.2 dB/km at 1550 nm. At wavelengths higher than this the loss increases rapidly due to optical absorption in the fiber material. The interference effect of Rayleigh backscattering is used in the ϕ-OTDR to detect intruders.

Another issue which affects the performance of the intrusion sensor is the polarization of the Rayleigh backscattering. The optical fibers do not generally maintain the polarization state of the input light for more than a few meters due to birefringence that varies randomly throughout the length of the fiber. Single mode fibers with nominal circular symmetry about the core axis allow the propagation of two nearly degenerate modes with orthogonal polarizations. The different phase velocities of the

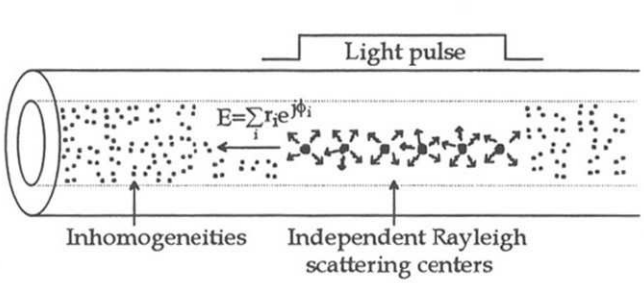

Fig. 4. Rayleigh scattering in an optical fiber

two modes results in a phase difference between the two modes after a certain length of fiber. Thus, the polarization state of the light will change between linear, circular and elliptical due to this effect. The ϕ-OTDR is very sensitive to the polarization state of the backscattered light.

C. Phase Sensitivity of a Buried Fiber

The sensitivity of a buried fiber optic cable to the pressure of an intruder walking over it is an important factor for achieving a practical intrusion detection sensor. Even though it is possible to calculate the phase shift due to lateral pressure on a fiber, such calculations do not adequately account for the influence of the cable itself and the surrounding soil composition and conditions. Therefore, experiments were undertaken at the Texas A&M University to measure the phase change produced by the pressure due to weight of an intruder above the buried fiber cable.

Experiments were conducted to analyze the phase shift produced in the fiber cable buried in a sand box when pressure was applied on the cable. The buried cable was spliced into one arm of an all-fiber Mach-Zehnder interferometer. A box with dimensions 30 cm x 10 cm (approximately the size of a human foot) was placed directly above the buried cable, and weights were added to the box to produce a

π-radian phase shift as determined by monitoring the interferometer output power. It was observed that for a depth of 20 cm a 60 kg intruder produced a phase change of about 6π radians, while for a 40 cm depth the phase change was about 2.4π radians. It was found that for a give burial depth the induced phase change was a linear function of the applied weight [9].

Further investigations were made to determine if it was possible to avoid detection by stepping over the sensor cable. Fiber was buried at a depth of 30 cm in clay soil and it was found that a 60 kg intruder produces a π-radian phase shift within 2 m on either side of the buried cable and several π-radian phase shifts when directly over the cable. It was also observed that seismic signals produced in the earth by a moving motor vehicle could be sensed by the buried interferometer. These experiments indicated that a commercial fiber optic cable is suitable as the sensing element for a fiber optic intrusion sensor system [10].

D. OTDR

Optical time domain reflectometry (OTDR) is a sophisticated measurement technique which finds application in both laboratory and field for the characterization of attenuation, imperfections and splicing locations in long lengths of fibers. The main applications of OTDR are measurements of splice loss, connector loss, microbending loss, diameter fluctuation and fiber length [11]. A block diagram of a typical OTDR is as shown in Fig. 5 [12]. A light pulse is launched into the fiber by a pulsed laser through a directional coupler. The backscattered light is detected using a photodetector and is passed through a signal processing unit and then observed using an oscilloscope. The backscatter plot is illustrated in Fig. 6 [7]. The detected optical power decreases exponentially with the distance along the fiber. Losses due to the

discrete reflection from a fiber joint as well as a discontinuity due to excessive loss at a fiber imperfection or fault and Fresnel reflection are observed as abrupt peaks. The conventional OTDR however does not respond to phase modulation of the light as the spectral width of the laser is very broad (GHz to THz range).

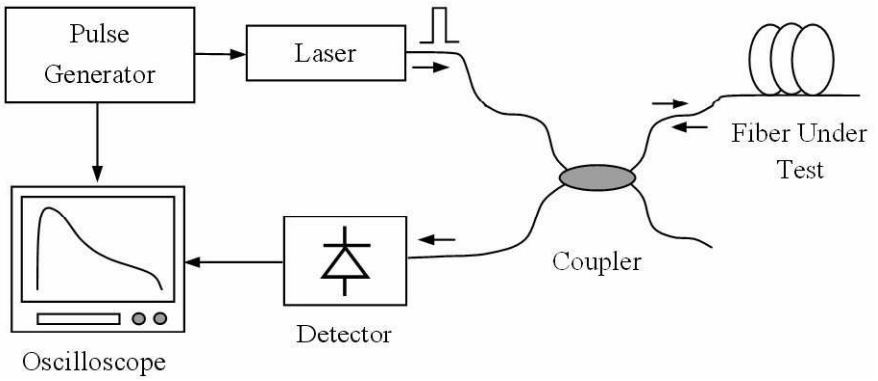

Fig. 5. Block diagram of conventional OTDR

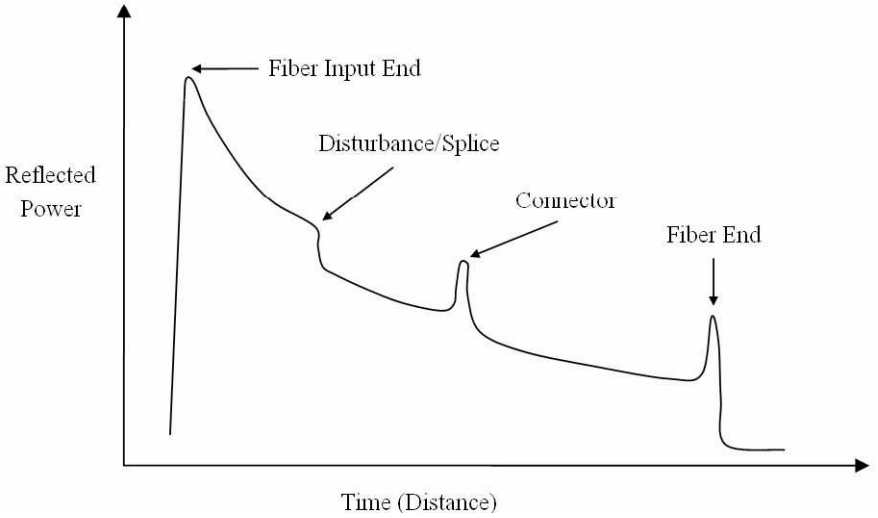

Fig. 6. Typical OTDR trace

E. Phase-sensitive OTDR for Intrusion Sensor

In the perimeter intruder sensor investigated in the Texas A&M University, phase changes produced by the pressure of the intruder on the ground above the sensor and the seismic disturbances caused by moving vehicles in the vicinity are sensed by a phase sensitive optical time domain reflectometer (ϕ-OTDR). The ϕ-OTDR enhances the coherent effects that have higher sensitivity to the environmental perturbation than the intensity based sensors such as a conventional OTDR where coherent effects are minimal due to the broad spectral width of the laser. The phase sensitivity of the ϕ-OTDR is due to the interference of the Rayleigh backscattered light which arrive simultaneously at the photodetector. In case of the conventional OTDR this interference is mostly avoided as the spectral width of the modulated laser is very broad (GHz to THz range). The ϕ-OTDR uses a very narrow linewidth laser to enhance the coherent effects [5] [13] [14].

The back scattered fields of each reflecting center within the pulse width interfere with each other at the photodetector, as a light pulse travels along the fiber. If a perturbation occurs in certain part of the fiber, it manifests itself as a change in the refractive index or length of the fiber. The backscattered light downstream from the perturbation in the fiber experiences a round-trip phase shift as it passes through the perturbation twice. Therefore, the resultant intensity of the interference from the Rayleigh scattering centers will be changed at a time corresponding to the location of the perturbation [4]. This is given by eq. 2.2, where T is the duration of the return pulse, L the length of the fiber, n_g the refractive index of the fiber and c the free space speed of light. Thus, when an intruder steps on the sensing cable or seismic perturbations are caused by moving vehicles in the vicinity of the sensor, a phase change is produced in the light pulse.

$$T = \frac{2Ln_g}{c} \tag{2.2}$$

If both the light source and sensing fiber are stable, then the OTDR trace will be affected at the point of perturbation and will remain stable in time at the rest of the locations. By subtracting the trace with the perturbation from a perturbation free trace, the intruder can be detected and located as illustrated in Fig. 7 [3].

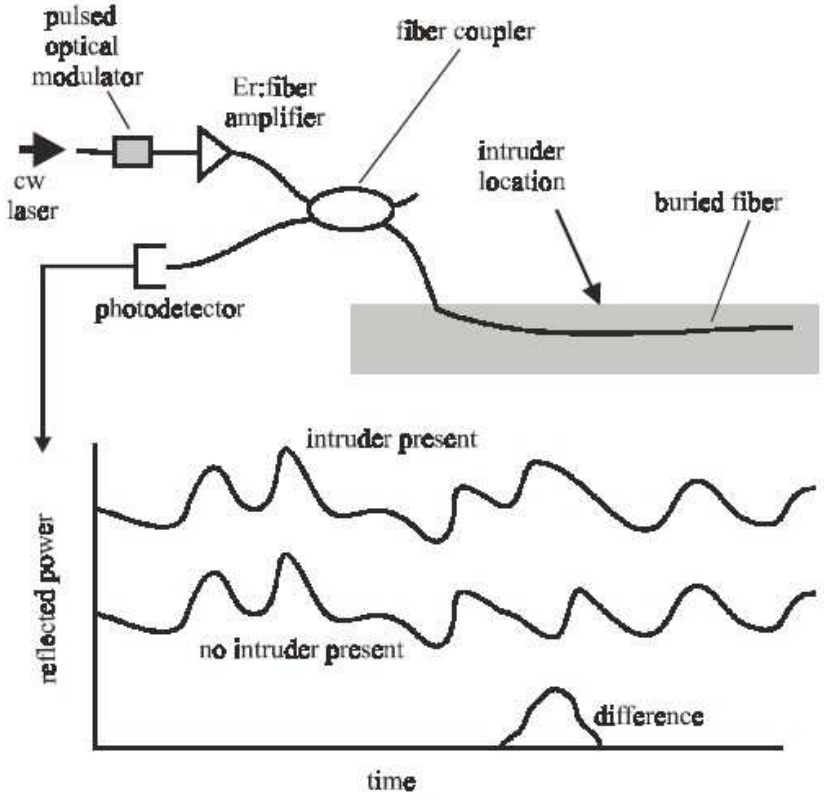

Fig. 7. Configuration of ϕ-OTDR intrusion sensor

For a silica fiber with $n_g = 1.46$, it is calculated that T = 9.73 L, with T in μs and L in km. Thus, for a 20 km fiber, the duration of the return signal is 195 μs. Simulation were performed to study the response of the ϕ-OTDR to phase perturbations. The Monte Carlo method was used to set the random locations of the

scattering centers in the fiber. The dependence of range resolution on the detection range based on theoretical calculations is given by Fig. 8 [3].

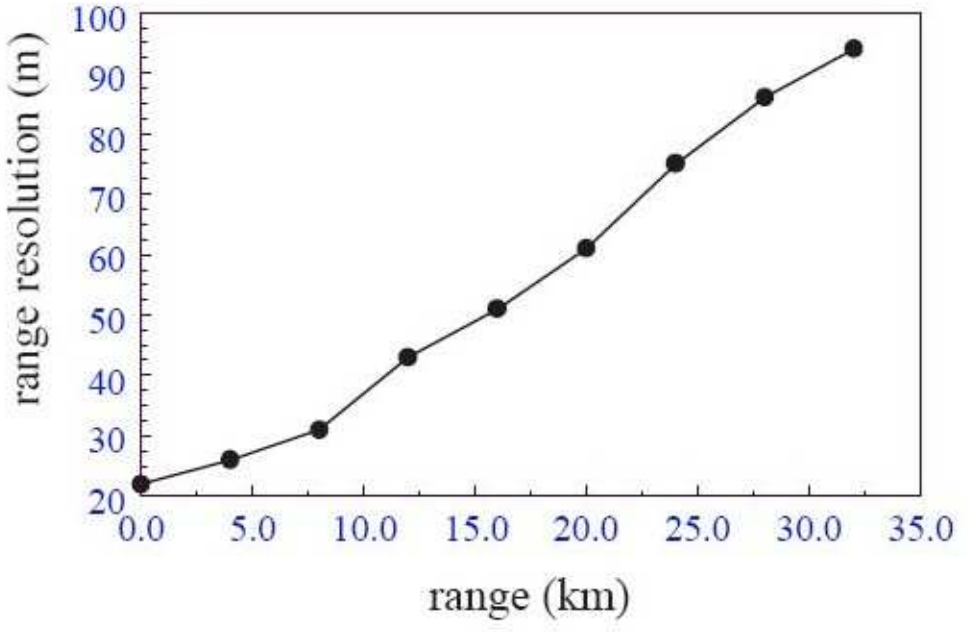

Fig. 8. Simulated dependence of range resolution on detection range of fiber

F. Er:Fiber Laser

For the the implementation of the fiber intrusion sensor based on the principle of ϕ-OTDR a highly stable laser with very low frequency drift and a narrow instantaneous linewidth is required. A spectrally stable Er:Fiber laser was developed in the Texas A&M University for practical application in the ϕ-OTDR [5]. This laser was successfully used in a practical implementation of a distributed fiber-optic sensor [3] . However, substantial improvements were required in the frequency drift and the sensitivity to acoustic and outside environmental conditions were required before further field tests could be performed.

The improved Er:doped fiber laser with narrow linewidth, low frequency drift and high stability used in the current intrusion sensor is as illustrated in Fig. 9. This fiber laser utilizing all single mode fiber paths consists of two Fiber Bragg Gratings (FBG) with reflectance peaks at 1555.4 nm and spectral widths of 0.4 nm. These FBG form the Fabry-Perot cavity. The reflectances are 99.99% at the back side and 92% at the output side. The gain medium is a 3 m long Er+3 doped fiber (18 dB/m gain) pumped by a 980 nm semiconductor pump laser through a wavelength division multiplexing (WDM) coupler. A small feedback loop (∼1 m) is provided using 90/10 optical directional couplers to improve the spectral characteristics of the laser. Two optical isolators at the immediate output of the Fabry-Perot cavity prevent any back emission of the laser and make the feedback loop unidirectional. The output power of the laser is 500 μW at 1555.4 nm as shown in Fig. 10 [12]. The laser is housed in a thermally and acoustically insulated enclosure to ensure stable operation of the laser.

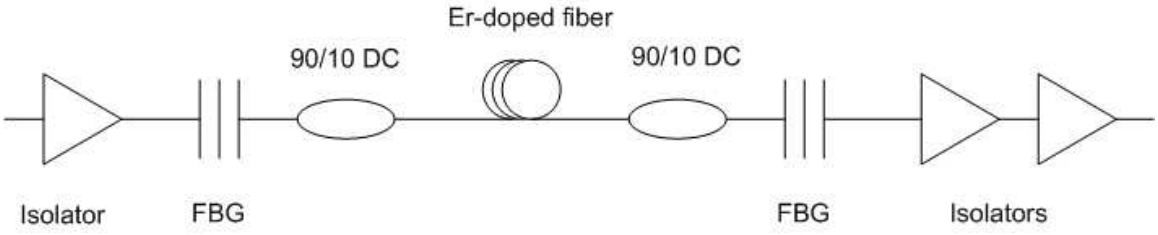

Fig. 9. Setup for Er:doped fiber laser

G. Laser Linewidth Measurements

The ϕ-OTDR requires a laser having narrow instantaneous linewidth $\ll 1/\tau$ where τ is the laser pulse width to be sensitive to phase changes along the fiber. Conventional spectrum analyzers do not have the required resolution to measure such narrow

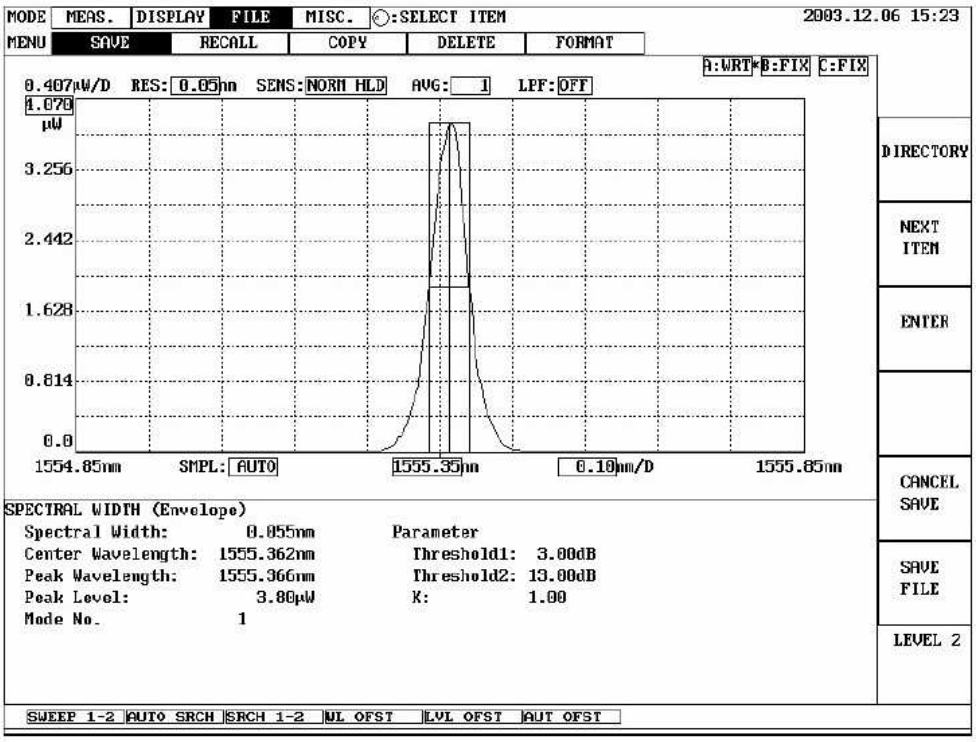

Fig. 10. Spectral linewidth scan of Er:doped fiber laser

linewidths. Hence, a delayed self-heterodyne setup consisting of a fiber Mach-Zehnder interferometer with a 63 km delay line in one arm was used for the instantaneous linewidth measurement of the laser [12] [15].

H. Frequency Drift Measurements

An all-fiber Mach-Zehnder interferometer was used to characterize the frequency drift of the Er:laser. The rate of the frequency drift was measured by observing the temporal fringes in a pair of Mach-Zehnder interferometers (MZI) with path length differences of 200 m. Both the MZIs were housed in insulated surroundings to reduce the effect from environmental perturbations. Under normal conditions, a frequency drift of ∼1-1.5 MHz/min were observed. Under the quietest conditions, a frequency drift of ∼100-300 KHz/min were observed. Under the most stable and quietest environmental conditions, the laser was found to operate in a single longitudinal mode with occasional mode hops and with a frequency drift approaching 1 KHz/min, which is better than needed for the successful operation of the intrusion sensor [2].

CHAPTER III

EXPERIMENTAL SETUP AND PROCEDURE

A. OTDR Setup

Once the laser was stabilized the performance of the ϕ-OTDR was investigated in a laboratory setting. The effect of the intruder walking over the fiber was simulated using a PZT consisting of about 10 m of fiber wound on a piezoelectric cylinder. Data was acquired using a digital oscilloscope and then transferred to a desktop computer. This data was processed by a LabView program [12]. This setup was modified for better performance and is as shown in Fig. 11.

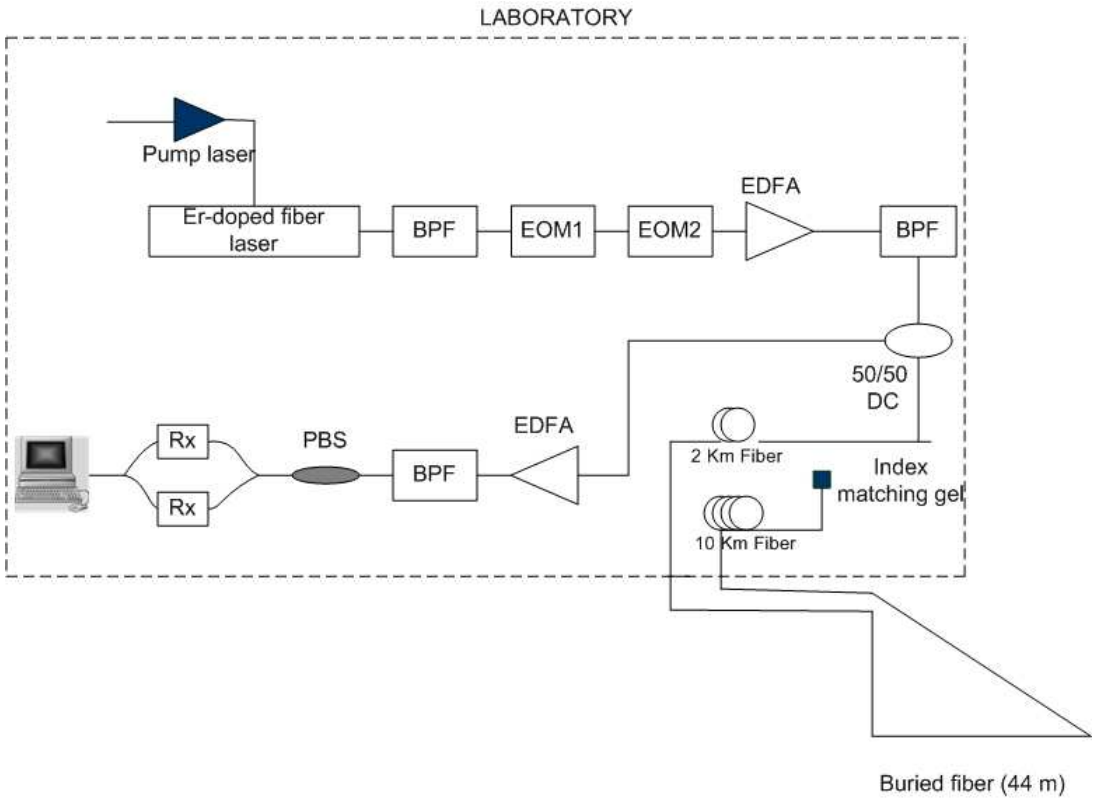

Fig. 11. Field test setup for characterizing the ϕ-OTDR system

The current experimental setup is at the Riverside campus of the Texas A&M University. The setup consists of a pump laser that drives the Er:doped fiber laser and light from this laser passes through a Band Pass Filter (BPF) to remove spontaneous emission. The light pulses are then modulated to the desired frequency using Electro Optic Modulators (EOM). The output from the EOM is then amplified by ∼30 dB using an Er:doped Fiber Amplifier (EDFA) and again filtered using a BPF. The light coming out of this BPF is then coupled into the sensing arm of the fiber using a 50/50 optical Directional Coupler (DC). The intrusion sensor is simulated using 12 km of fiber which is made of two spools of fiber (2 km and 10 km) with the sensing arm spliced in between them. The width of the laser pulse entering the fiber is 2 μs with a spatial resolution of 200 m. The sensing arm consists of 44 m of 3mm-diameter single mode fiber buried in a triangular path in clay soil. The 44 m of fiber passes out through a conduit in the wall of the laboratory in which all the monitoring equipments are housed. It is then laid out in a triangular path in clay soil at depths of 8 inches (20.32 cm) to 18 inches (45.72 cm) in a 10.16 cm wide trench as shown in the Fig. 12 [12]. The cable was buried in July, 2002 and the soil has been naturally compacted over the two years. The reflected light is passed through a 3 dB coupler and an EDFA is used to boost the signal at the receiver end. A Polarization Beam Splitter (PBS) is used to split the light into two orthogonal polarizations and process them separately. Two photodetectors operating 20 dB gain are used for the two polarizations. This setup provides a higher signal-to-noise ratio (SNR) in the receivers and reduce the "fading" effect. A National Instruments PCI-6111 card was used for acquiring the data at 5 MSample/s. The collected data is then processed in a desktop computer.

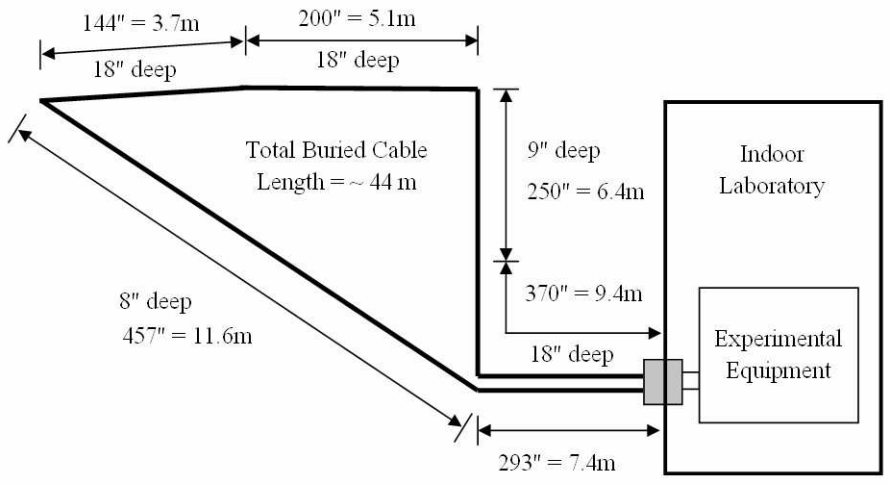

Fig. 12. Configuration of buried sensor

B. Experimental Procedure for Sensitivity Analysis

The sensor to be tested consists of the 44 m of single mode fiber optic cable buried in the clay soil outside a laboratory building at Texas A&M's Riverside Campus in northwest Brazos County. The laser and other monitoring equipment are located inside the building. The fiber is laid out in a triangular path and the buried fiber was divided into three sections for testing purposes, as illustrated in Fig. 12, and is connected to the equipment through a conduit in the wall of the lab. Tests were carried out in Fall 2004 and Summer 2005.

The series of tests were carried out to investigate the response of the sensor to intruders on foot and vehicles. Test were conducted to study the response of the sensor to different situations and also to evaluate the reliability of the sensor. The data on the sensor response was recorded as a person walked perpendicular to the sensor line at three different locations in each section of the triangular path, as shown in Fig. 13. This test provided information on the falloff in sensor response with lateral distance and on the largest distance at which a signal can be observed. People

of weights ranging from 135 lbs (∼63 kg) to 195 lbs (∼91 kg) were employed in this study.

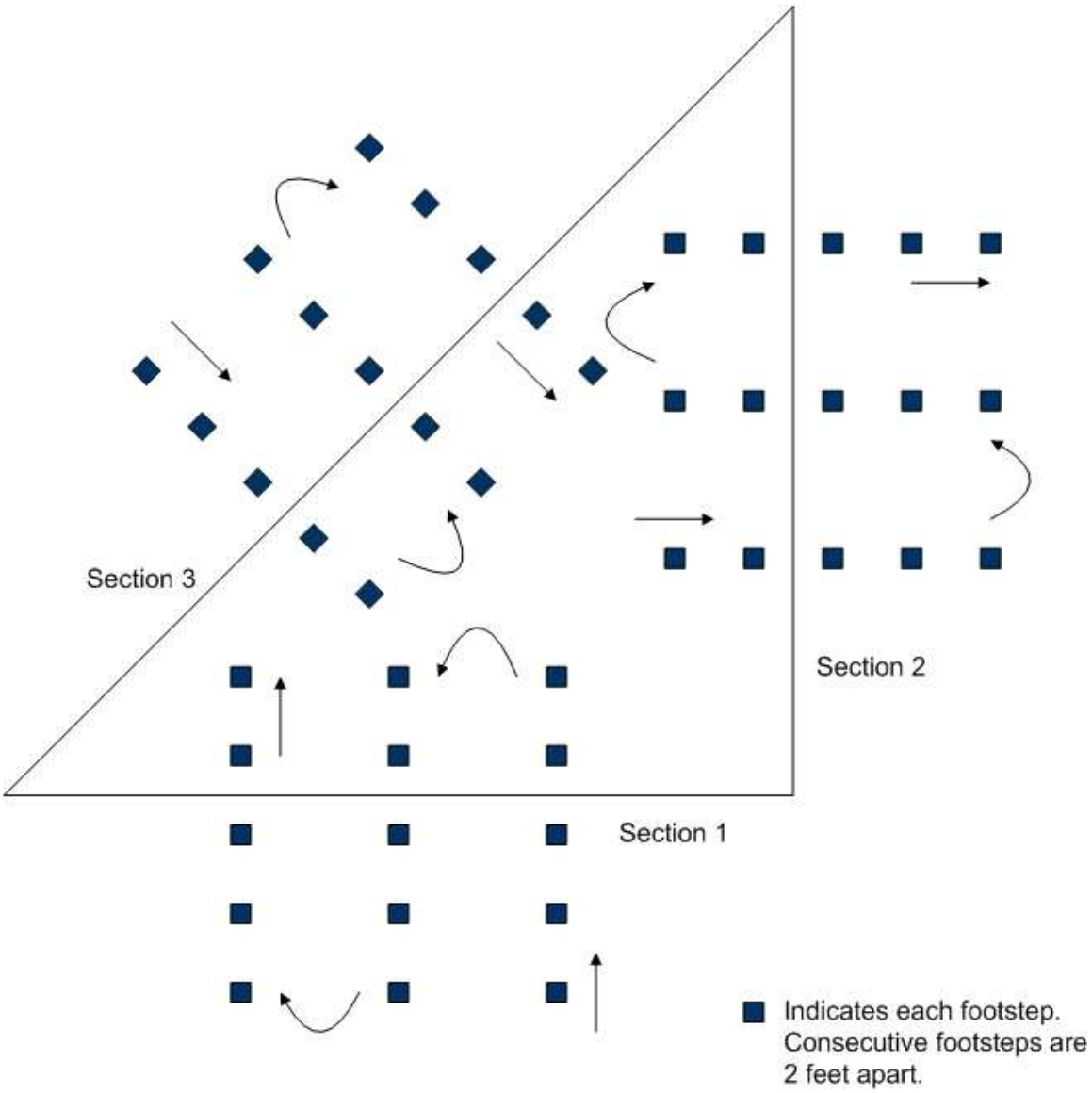

Fig. 13. Schematic of the test region and procedure

Another series of tests was conducted to determine the sensor's ability to detect motor vehicles driving in the vicinity, as shown in Fig. 14. The falloff in signal with the vehicle's distance and the maximum distance at which the sensor can sense the

seismic perturbations caused by the vehicle was determined. The effect of vehicle speed and of road condition (rough or smooth surface) was also studied.

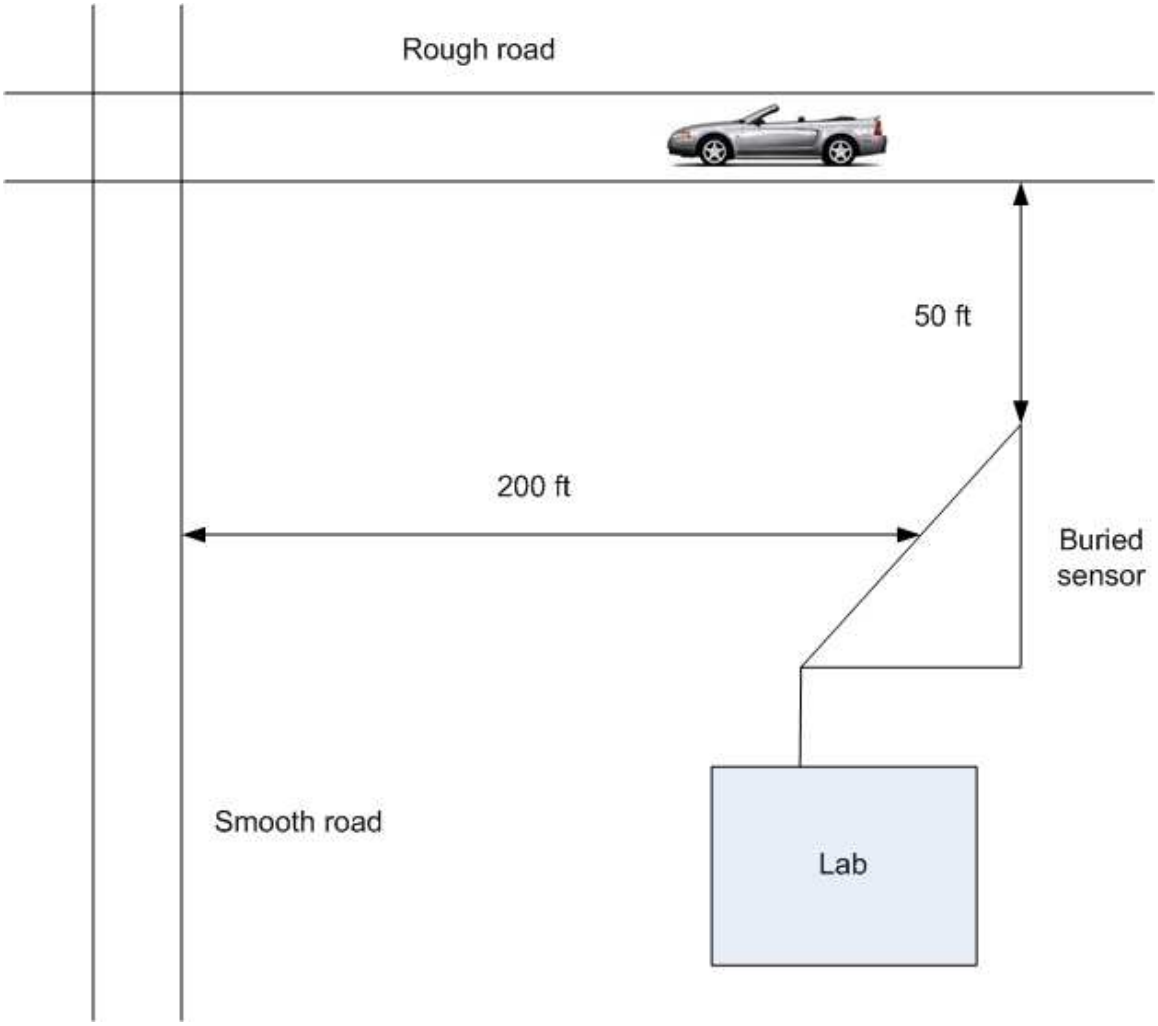

Fig. 14. Layout of the test setup for moving vehicles

The effect of an interfering signal from a vehicle on the ability to detect an intruder on foot was also investigated. The effect of the distance of the vehicle from the sensor, the road condition, and the speed and weight of the vehicle on the ability to observe the signal from an intruder on foot was characterized.

CHAPTER IV

RESULTS

A. Results for Intruders on Foot

Tests were performed to evaluate the sensitivity and repeatability of the sensor to intruders for each section of the buried fiber. A typical recording of the OTDR trace and the processed signal from the computer screen before the presence of the intruder and after a step has been taken by the intruder is as shown in Fig. 15 and Fig. 16. Each figure shows the ϕ-OTDR traces for both polarizations on the top trace and the processed signal on the bottom trace. For each such step taken by the intruder the signal strength is rated on a scale of one to ten. The difference waveform is observed at the 2 km point on the OTDR trace due to the pressure created by the intruder's step.

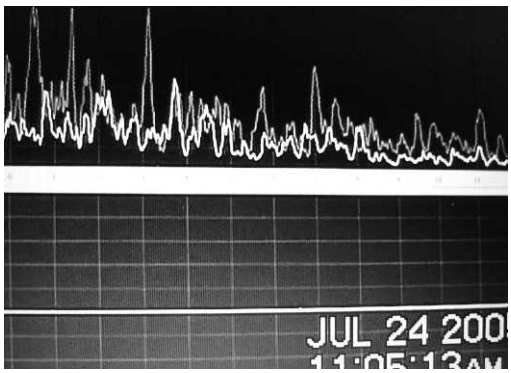

Fig. 15. PC screen capture showing OTDR trace on top and processed trace showing no signal at the bottom

1. Tests for Sensitivity and Repeatability: Nov. - Dec. 2004

These tests were conducted for two intruders, intruder 1 weighing 180 lbs (∼82 kg) and intruder 2 weighing 135 lbs (∼62 kg). Tests were repeated (60 - 90 times) on

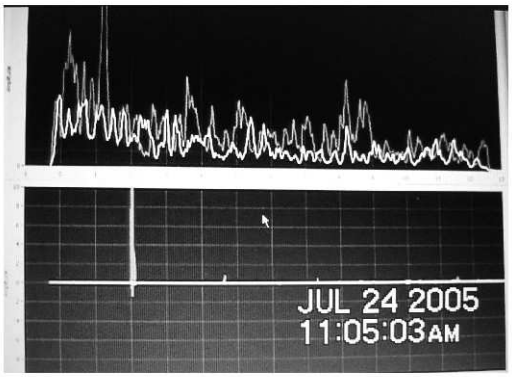

Fig. 16. PC screen capture showing OTDR trace on top and processed trace showing full-scale response at the bottom

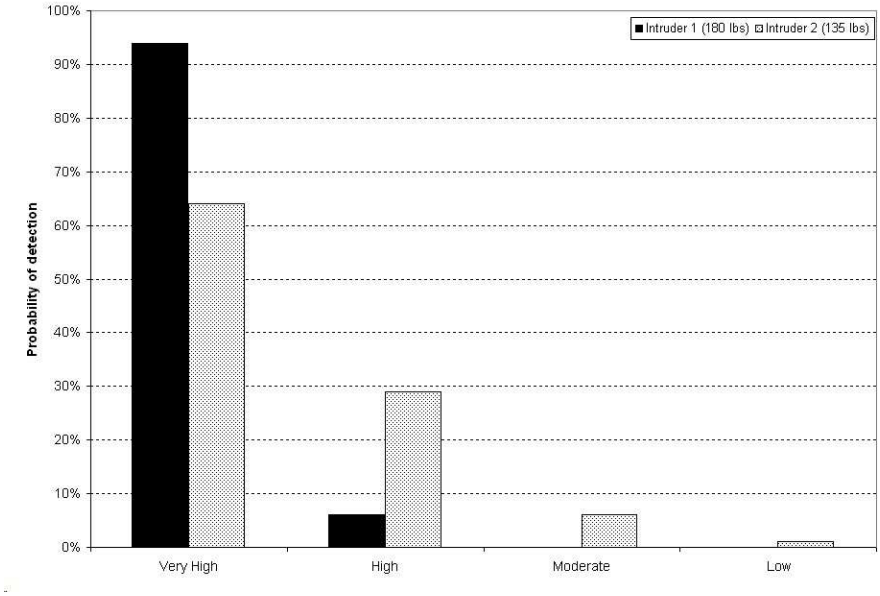

Fig. 17. Probability of detection of intruder 1 and intruder 2 in section 1; No. of trials for intruder 1 = 90 and for intruder 2 = 90. Probability of "Very High" or "High" signal level was 100% for intruder 1 and 92% for intruder 2

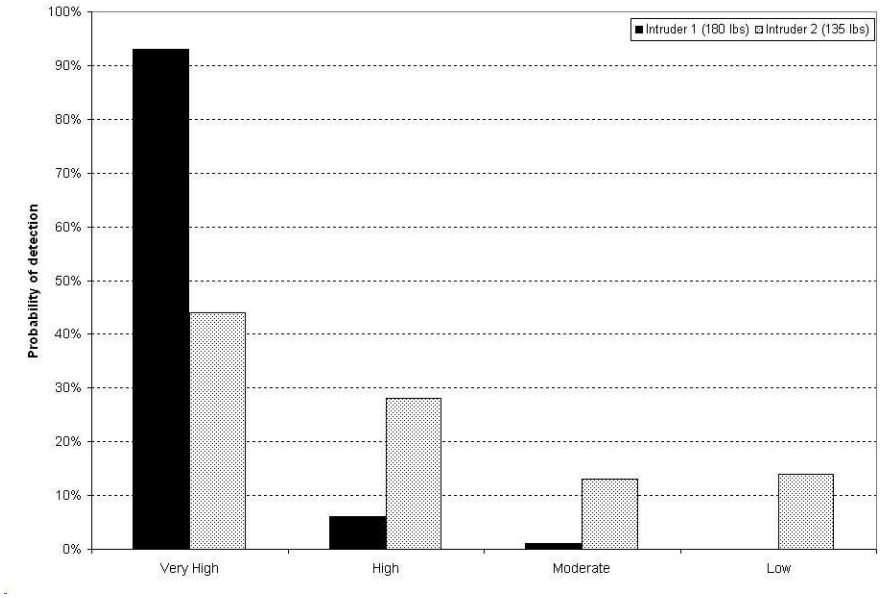

Fig. 18. Probability of detection of intruder 1 and intruder 2 in section 2; No. of trials for intruder 1 = 90 and for intruder 2 = 90. Probability of "Very High" or "High" signal level was 99% for intruder 1 and 73% for intruder 2

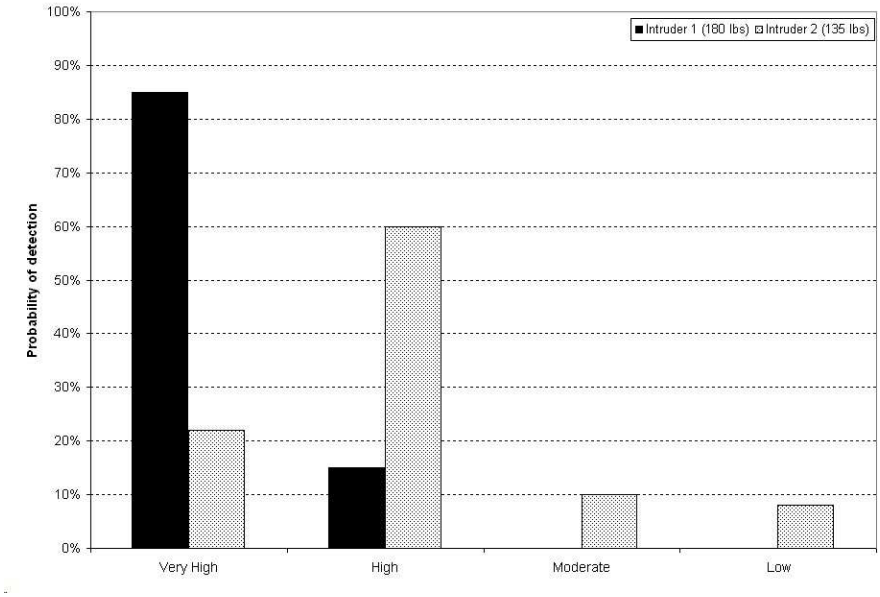

Fig. 19. Probability of detection of intruder 1 and intruder 2 in section 3; No. of trials for intruder 1 = 60 and for intruder 2 = 60. Probability of "Very High" or "High" signal level was 100% for intruder 1 and 83% for intruder 2

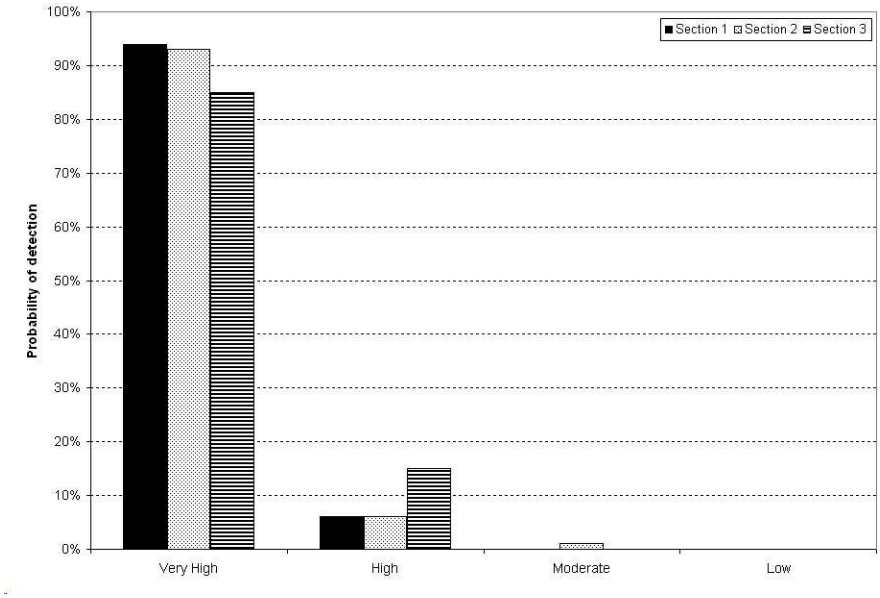

Fig. 20. Probability of detection of intruder 1 in sections 1, 2 and 3; No. of trials in section 1 = 90, section 2 = 90 and section 3 = 60

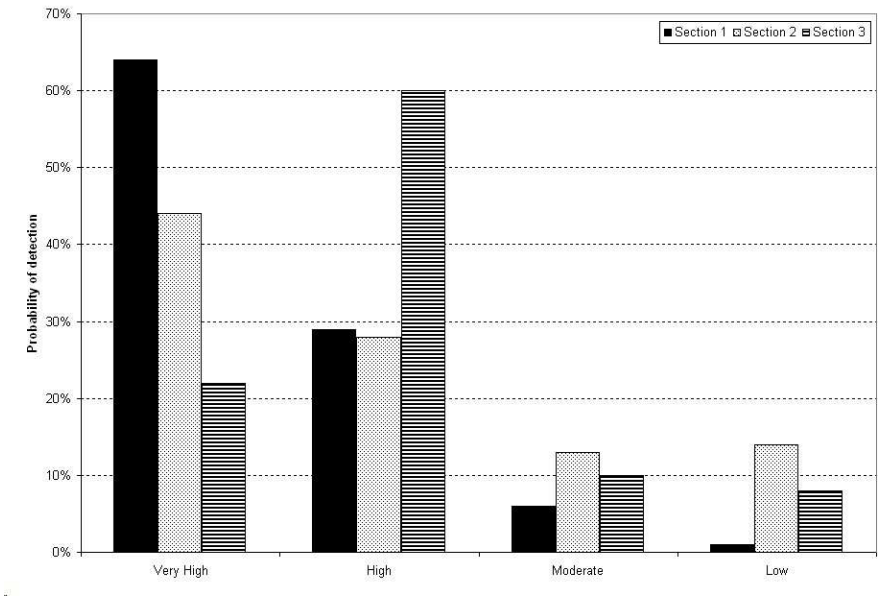

Fig. 21. Probability of detection of intruder 2 in sections 1, 2 and 3; No. of trials in section 1 = 90, section 2 = 90 and section 3 = 60

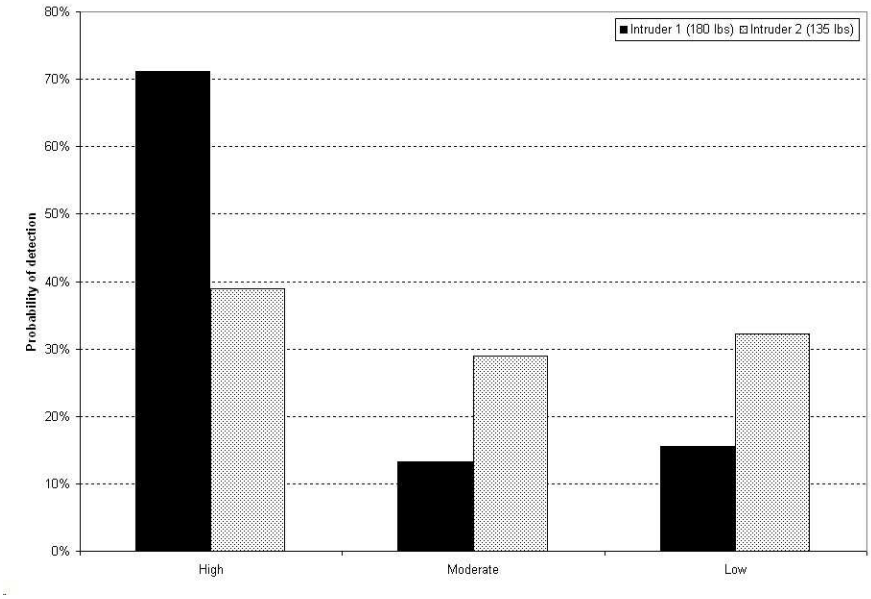

Fig. 22. Probability of detection at step no. 5 for intruders 1 and 2 in section 1; No. of trials for intruder 1 = 90 and for intruder 2 = 90

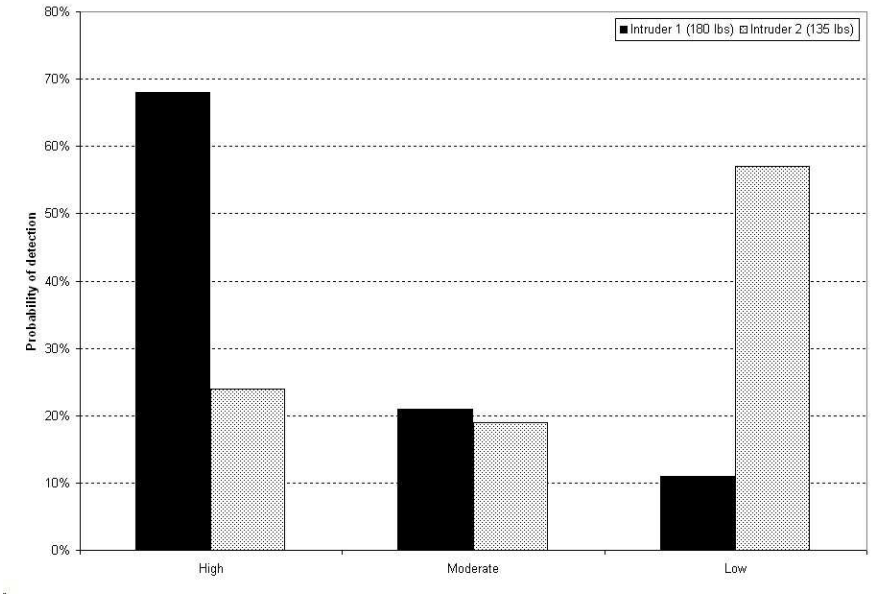

Fig. 23. Probability of detection at step no. 5 for intruders 1 and 2 in section 2; No. of trials for intruder 1 = 90 and for intruder 2 = 90

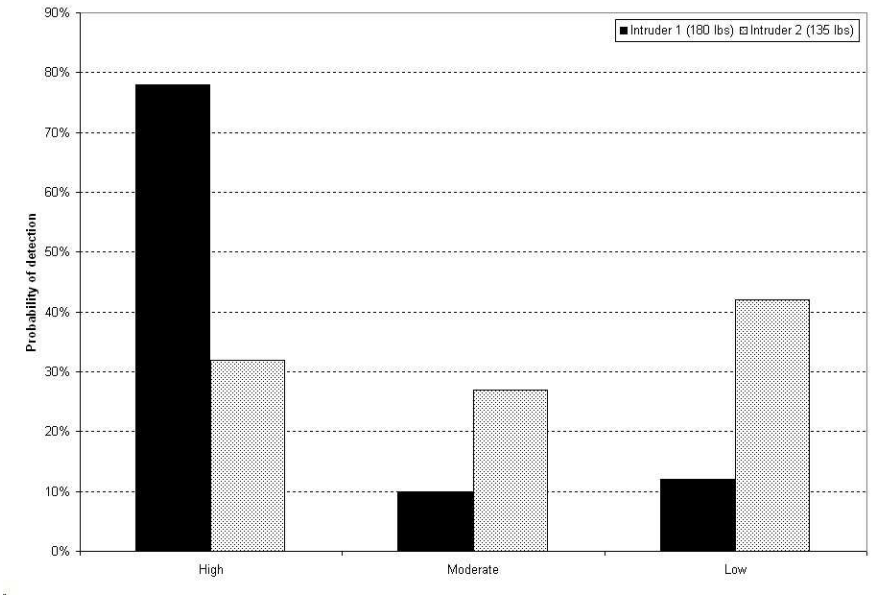

Fig. 24. Probability of detection at step no. 5 for intruders 1 and 2 in section 3; No. of trials for intruder 1 = 60 and for intruder 2 = 60

each of the three sections with both the intruders walking with a 2 ft gait. For each sequence of steps a total signal strength equal to the sum of the signal strengths for the five individual steps was calculated. Based on the total signal strength, the data was summarized into four categories. Total signal strength greater than 25 was classified as "Very High", between 10 and 25 was classified as "High", between 4 and 10 was classified as "Moderate" and less than 4 was classified as "Low".

The probability of detecting intruder 1 was significantly higher than that of intruder 2. This was because a higher pressure was produced on the ground due to intruder 1 weighing relatively more. Section 1 and Section 2 have more than 90% probability of detection as very high signal. The observations have been summarized in Fig. 17 to Fig. 21.

It was also observed that up to a distance of $\sim$5 ft from the sensor the probability of detection of the intruders was high on all the three sections. For distances less

than 5 ft the detection probability was very high and almost all the steps could be detected. This is as illustrated in the graphs (Fig. 22 - Fig. 24), where the probability of detection for a single step is classified on the basis of the signal strength. Signal strength of maximum value 10 was classified as "High", between 4 and 10 was classified as "Moderate" and less than 4 was classified as "Low".

2. Tests for Sensitivity, Repeatability and Lateral Range: Jul. - Aug. 2005

During the course of the sensor tests during the first half of 2005, it became evident that the sensor was responding to intruders at much greater distances from the buried cable than were studied in the Nov. - Dec. 2004 series of tests (See Figs. 17 - 24). It was therefore decided to carry out a new series of tests to obtain a better indication of the lateral range. The tests were conducted similar to what has been explained above but the intruder continued to walk for a total of 25 steps in a straight line, as illustrated in Fig. 25.

These tests were conducted on the Sections 2 and 3 of the buried sensor. Section 2 was tested by three intruders, intruder 1 weighing 195 lbs (∼91 kg), intruder 2 weighing 175 lbs (∼80 kg) and intruder 3 weighing 135 lbs (∼62 kg). Section 3 was tested by two intruders, intruder 1 weighing 195 lbs (∼88 kg) and intruder 2 weighing 135 lbs (∼62 kg). Fig. 26 - Fig. 29 summarize the results for the first five steps of each sequence using the same criteria for "Very High", "High", "Moderate" and "Low" detection probability that was applied in Fig. 17 - Fig. 21.

It was found that higher the weight of the intruder, higher was the probability of detection. Section 3 was more sensitive as its probability of detection was almost 100% for both the intruders (Fig. 26 - Fig. 29). The variation in sensitivity between sections is because of the depths at which the sensor is buried. Thus, section 3, where the fiber is buried at a shallower depth than section 2 shows higher probability of

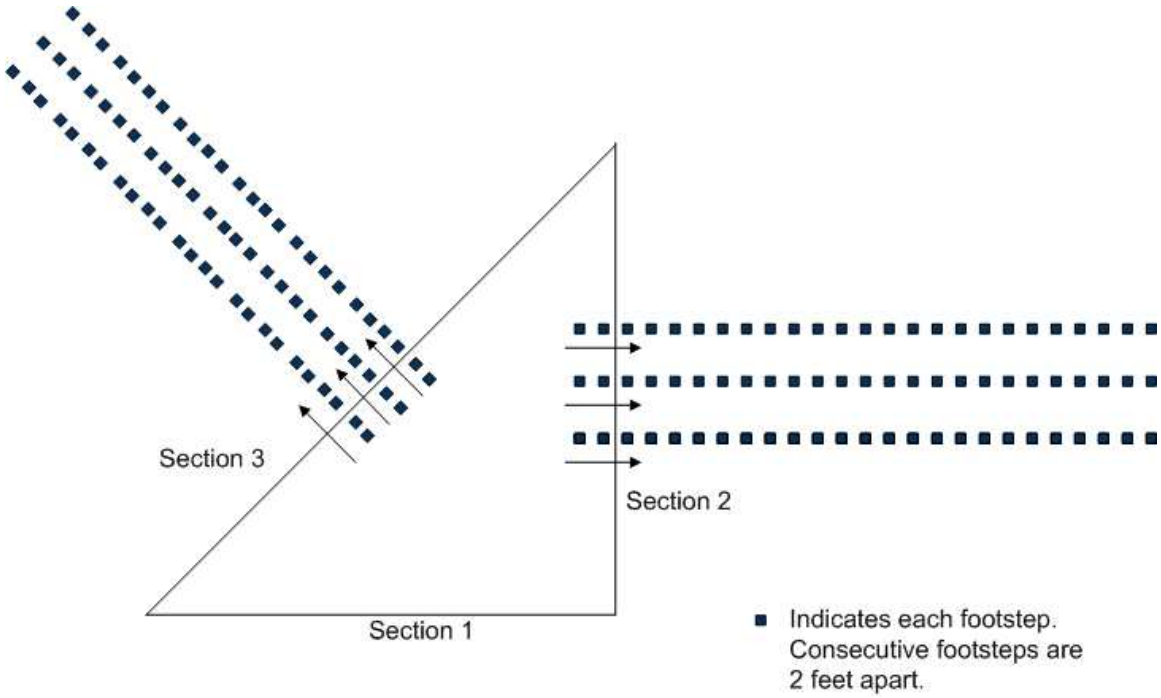

Fig. 25. Schematic of the lateral test region and procedure

detection.

In section 2, intruder 1 could be detected 40 ft away from the sensor, although the probability of detection was low. The probability of detecting a high (full-scale) signal was 17% for intruder 1 up to a distance of 17 ft from the sensor. For intruder 2 and intruder 3 the probability of detection was mostly low beyond 17 ft (Fig. 30 - Fig. 32). The probability of detection was maximum at the point where the intruder was crossing the sensor.

In section 3, for intruder 1, the sensor could detect a moderate (signal strength between 4 and 10) or high (maximum signal of 10) signal with 25% probability up to ∼37 ft away from the sensor. Similar to section 2, probability of detection was maximum at the point where the intruder was crossing the sensor. This is shown in the following graphs (Fig. 33 - Fig. 35).

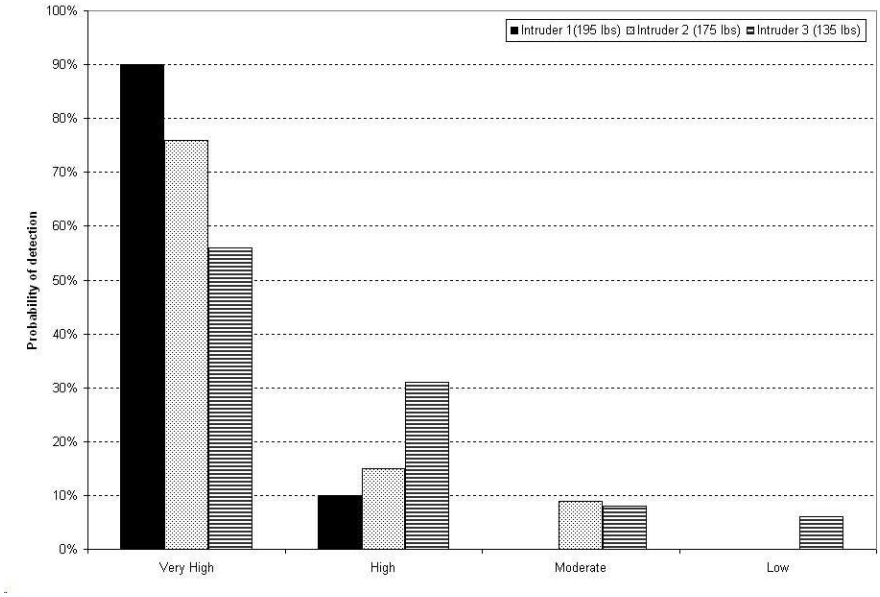

Fig. 26. Probability of detection of intruders 1, 2 and 3 in Section 2; No. of trials for intruder 1 = 69, intruder 2 = 33 and intruder 3 = 36. Probability of "Very High" or "High" signal level was 100% for intruder 1, 91% for intruder 2, and 85% for intruder 3

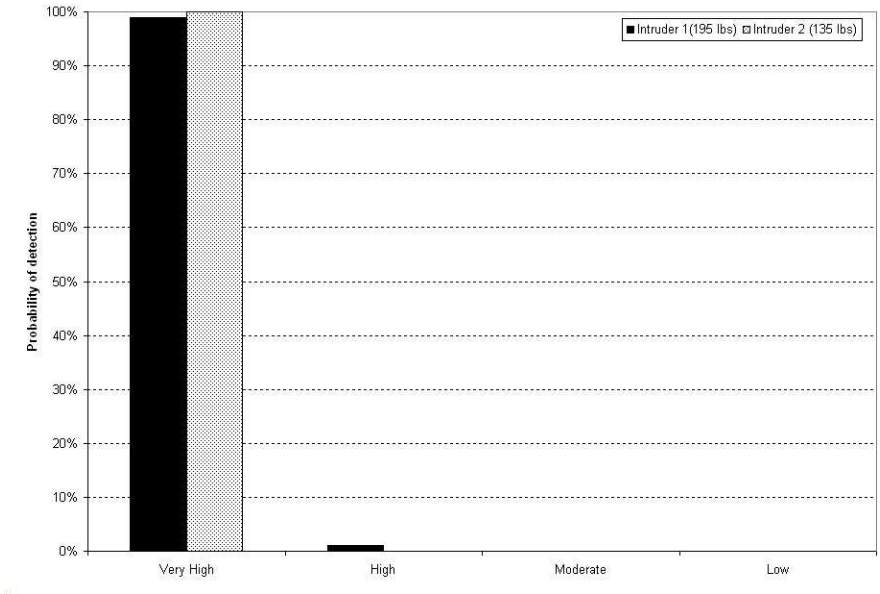

Fig. 27. Probability of detection of intruders 1 and 2 in section 3; No. of trials for intruder 1 = 129 and for intruder 2 = 10. Probability of "Very High" or "High" signal level was 100% for both intruder 1 and intruder 2

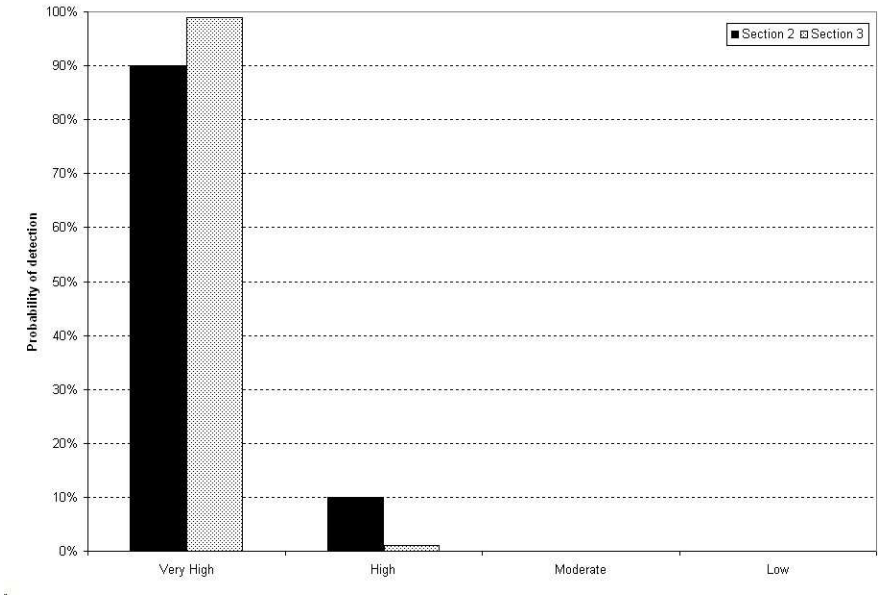

Fig. 28. Probability of detection of intruder 1 in sections 2 and 3; No. of trials in section 2 = 69 and section 3 = 129

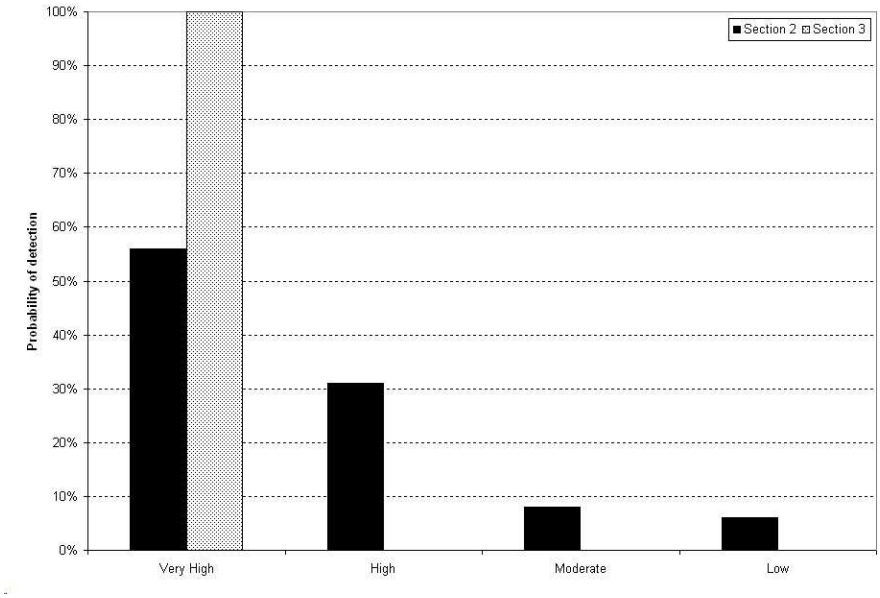

Fig. 29. Probability of detection of intruder 2 in sections 2 and 3; No. of trials in section 2 = 36 and section 2 = 10

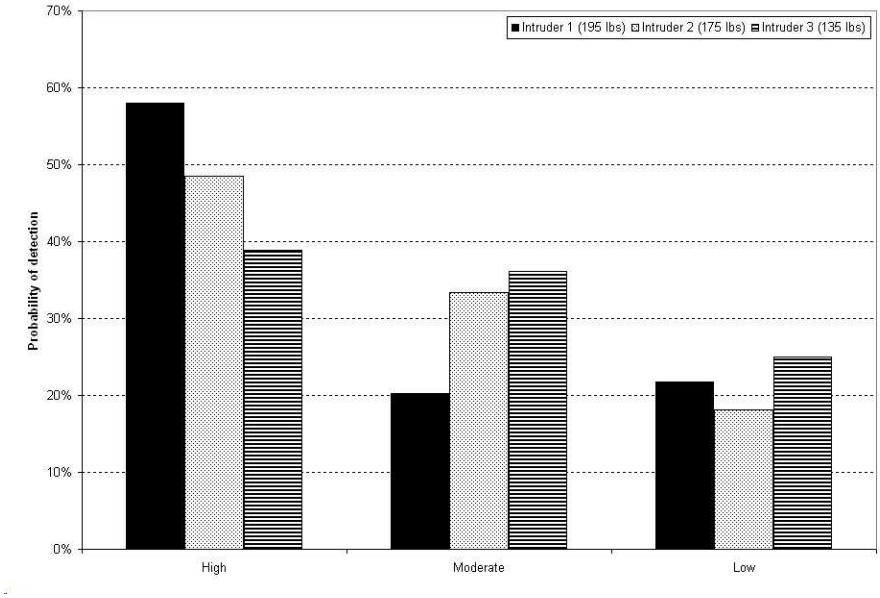

Fig. 30. Probability of detection at step no. 3 for intruders 1, 2 and 3 in section 2; No. of trials for intruder 1 = 69, intruder 2 = 33 and intruder 3 = 36

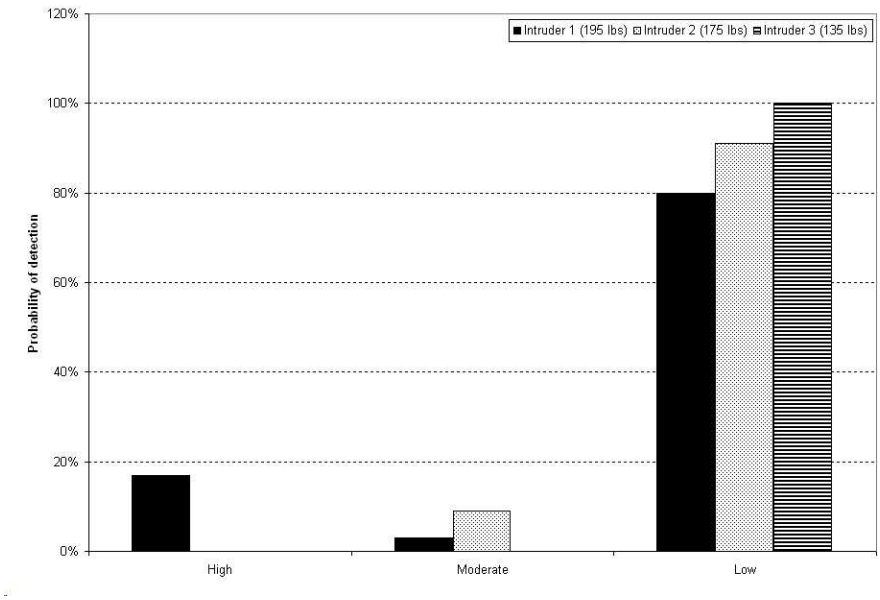

Fig. 31. Probability of detection at step no. 10 for intruders 1, 2 and 3 in section 2; No. of trials for intruder 1 = 69, intruder 2 = 33 and intruder 3 = 36

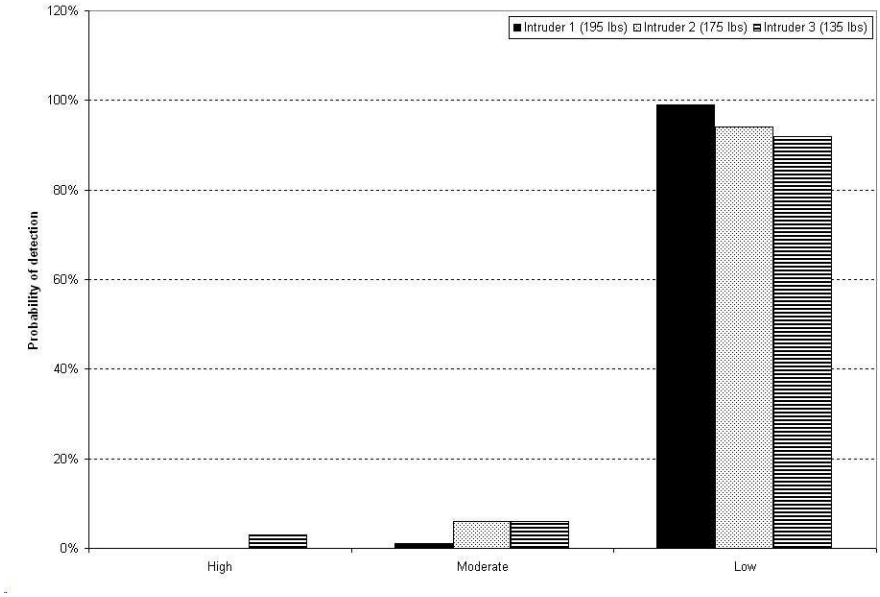

Fig. 32. Probability of detection at step no. 20 for intruders 1, 2 and 3 in section 2; No. of trials for intruder 1 = 69, intruder 2 = 33 and intruder 3 = 36

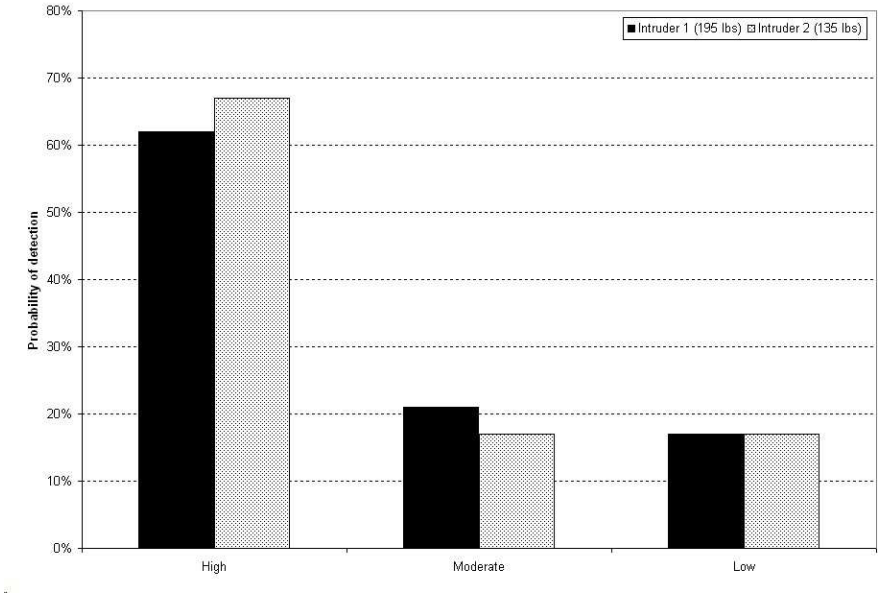

Fig. 33. Probability of detection at step no. 3 for intruders 1 and 2 in section 3; No. of trials for intruder 1 = 129 and for intruder 2 = 10

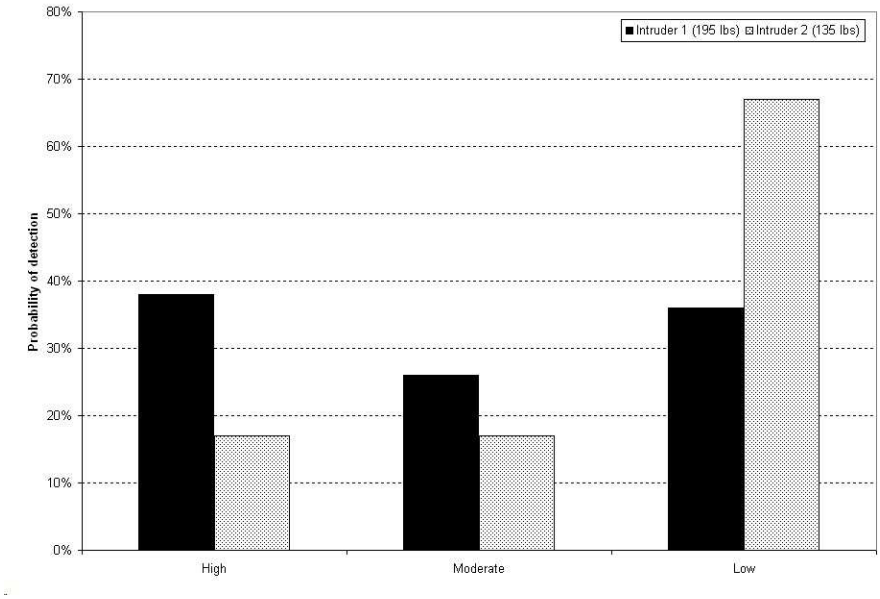

Fig. 34. Probability of detection at step no. 10 for intruders 1 and 2 in section 3; No. of trials for intruder 1 = 129 and for intruder 2 = 10

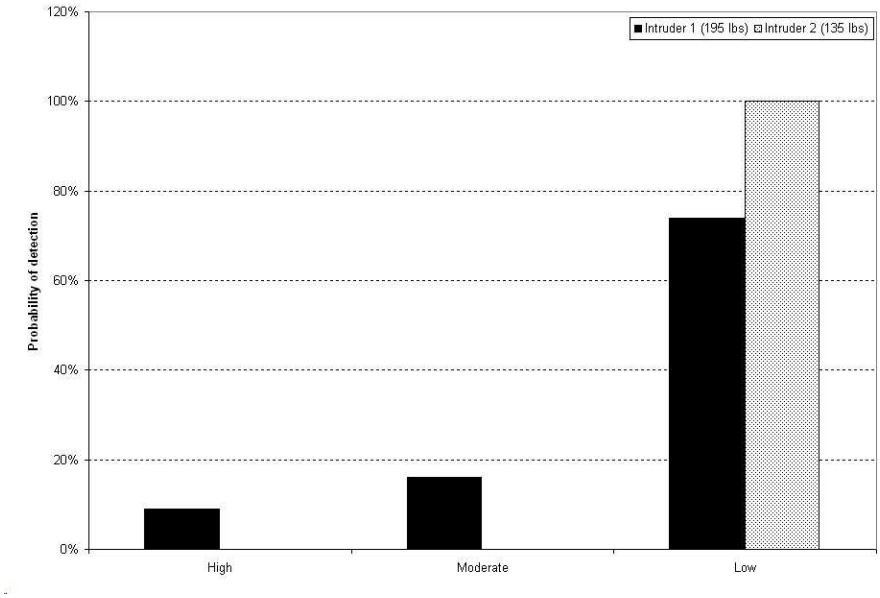

Fig. 35. Probability of detection at step no. 20 for intruders 1 and 2 in section 3; No. of trials for intruder 1 = 129 and for intruder 2 = 10

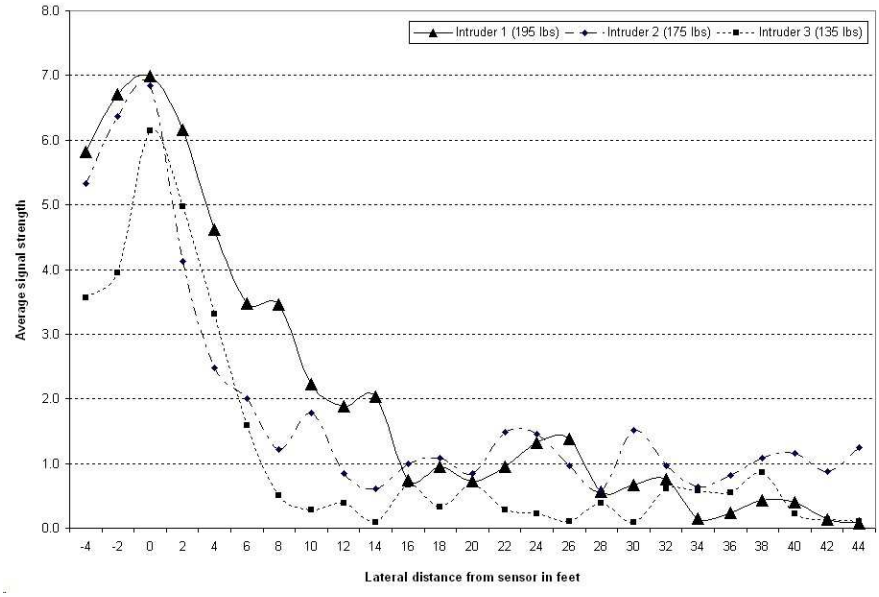

Fig. 36. Signal strength vs. lateral distance in section 2 for intruders 1, 2 and 3; No. of trials for intruder 1 = 69, intruder 2 = 33 and intruder 3 = 36

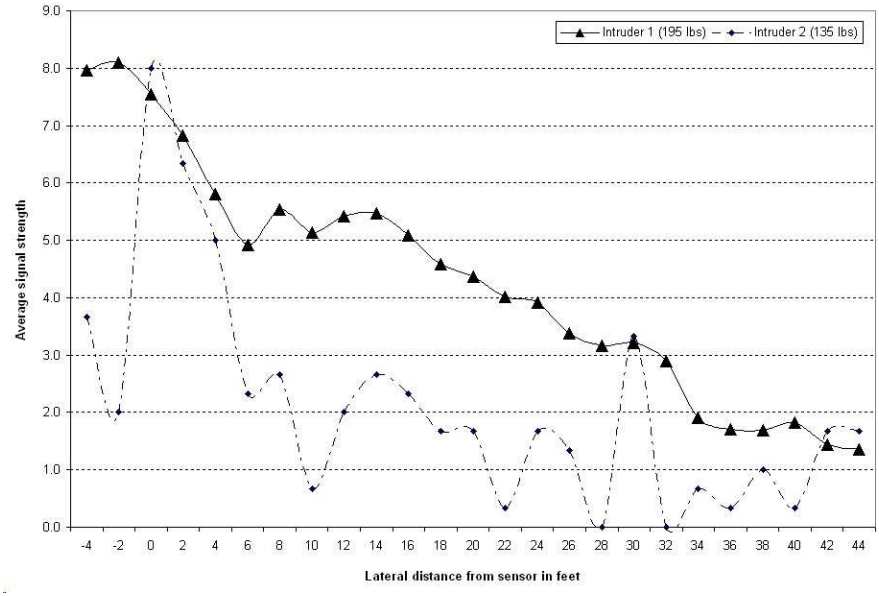

Fig. 37. Signal strength vs. lateral distance in section 3 for intruders 1 and 2; No. of trials for intruder 1 = 129 and for intruder 2 = 10

The average signal strength is plotted as a function of lateral distance from the cable line for sections 2 and 3 in Figs. 36 and 37, respectively. In the data of Fig. 36, the average signal level has fallen by a factor of 2 from the maximum at a distance of about 5 ft, and the signal level at 40 ft is about 10% of the maximum.

B. Results for Moving Vehicles

In this series of tests, the system response was observed on the computer screen as a car (weighing about 2700 lbs) was driven along the road in the vicinity of the sensor. In case of a moving vehicle the phase change is observed from the seismic perturbations produced when the car is driven over imperfections and rough patches on the road.

1. Test on Rough Road

The layout of the roads on which the car was driven is as shown in Fig. 14. This series of tests were performed on the unpaved road which passes about 50 ft from the nearest point of the sensor. The car was driven at the speeds of 10 mph, 15 mph, 20 mph and 30 mph. It was observed that higher the speed of the car longer the distance up to which it could be seen on the sensor. This is because the seismic disturbances caused by a fast moving vehicle is higher than that caused by a slow moving one. As seen from the Fig. 38, the car could be detected only up to a distance of $\sim$200 ft when moving at a speed of 10 mph while it could be seen up to a distance of $\sim$482 ft when moving at a speed of 30 mph.

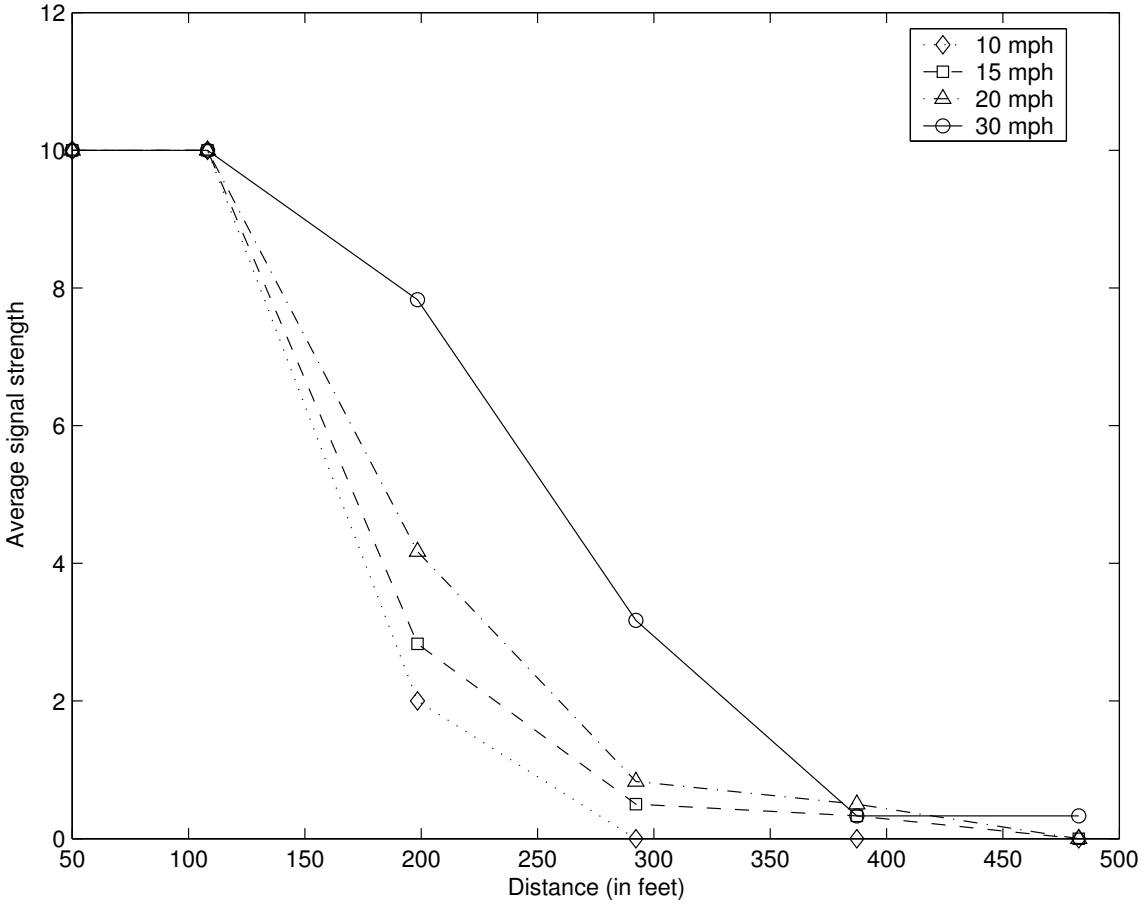

Fig. 38. Signal strength of car driven on rough road

2. Test on Smooth Road

This series of tests were performed on a paved road about 200 ft from the nearest point of the sensor. Again the car was driven at varying speeds of 10 mph, 15 mph, 20 mph and 30 mph. In case of the smooth road the car could be observed on the computer screen only when it drove through a rough patch in the road and otherwise could not be detected at all. The OTDR trace when the car was driven on the smooth road and when it was driven over a rough part of the smooth road is illustrated in Fig. 39 and Fig. 40.

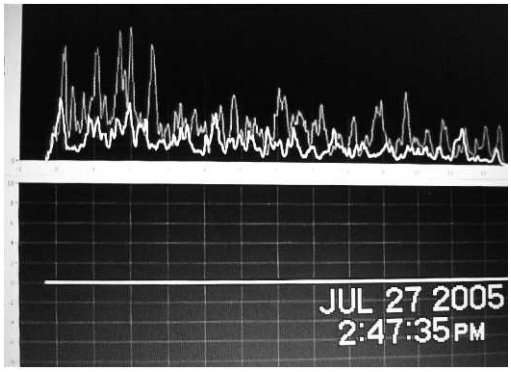

Fig. 39. PC screen capture showing OTDR trace on top and processed trace showing no signal at the bottom; when car was driven on smooth road at 20 mph

C. Results for Moving Vehicles and Intruder Simultaneously Present

The third series of tests were conducted to observe the interference from the moving car on the signal from the intruder on foot. The car was driven at speeds of 10 mph, 20 mph and 30 mph on the rough road and the intruder was made to walk on the sensor to produce maximum phase change. It was observed that when that car was driven at 10 mph, the signal produced by the intruder walking on the sensor could be observed after the car is ∼108 ft away from the sensor on the rough road. Similarly,

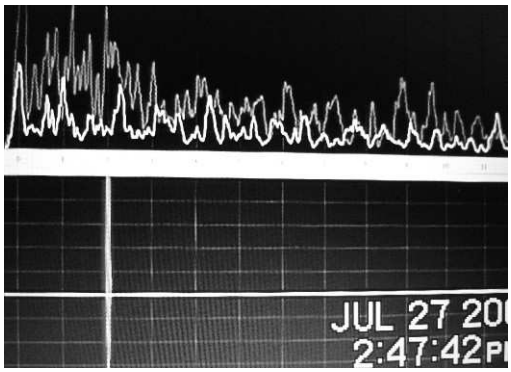

Fig. 40. PC screen capture showing OTDR trace on top and processed trace showing full-scale response at the bottom; when car driven on smooth road at 20 mph passed through a rough patch

for the higher speeds it was observed that the signal from the intruder on foot could be clearly distinguished once the car was ∼198 ft away from the sensor. These results are illustrated in Fig. 41 - Fig. 43.

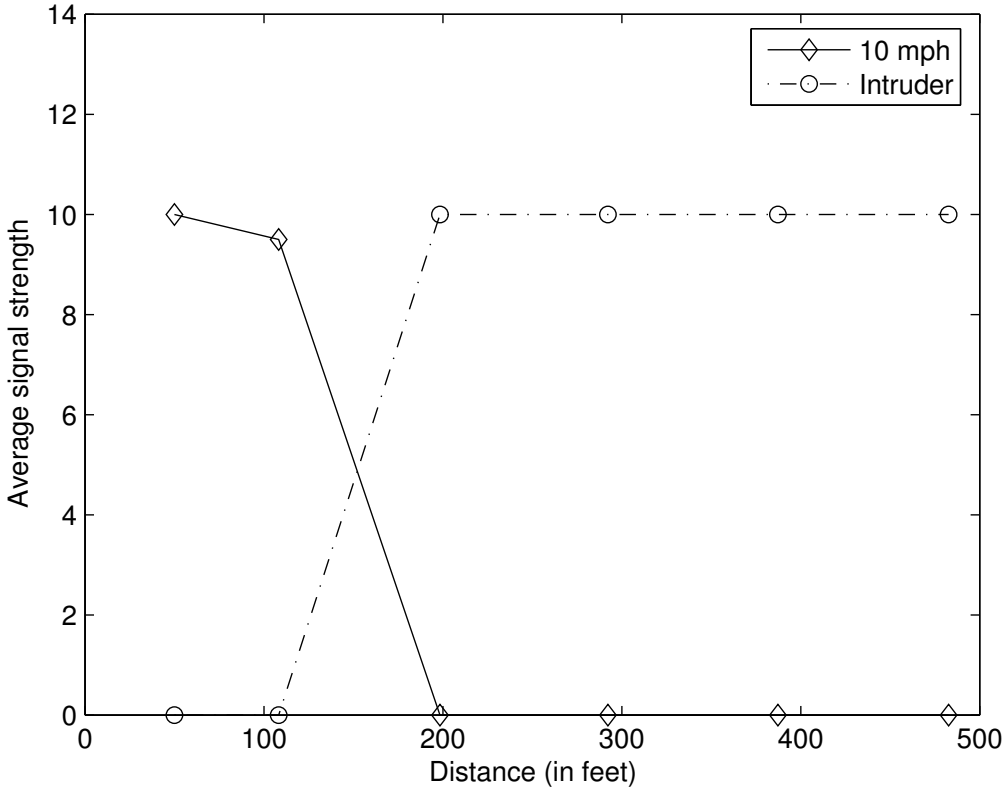

Fig. 41. Detection of intruder on foot while car driven at 10 mph on rough road

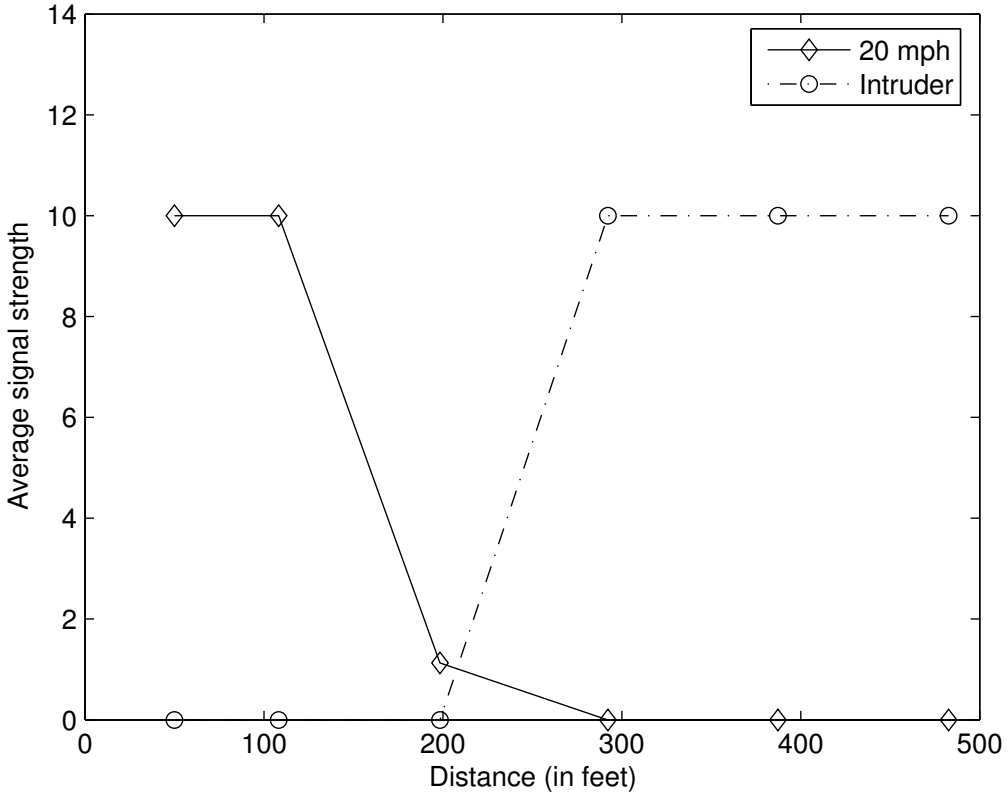

Fig. 42. Detection of intruder on foot while car driven at 20 mph on rough road

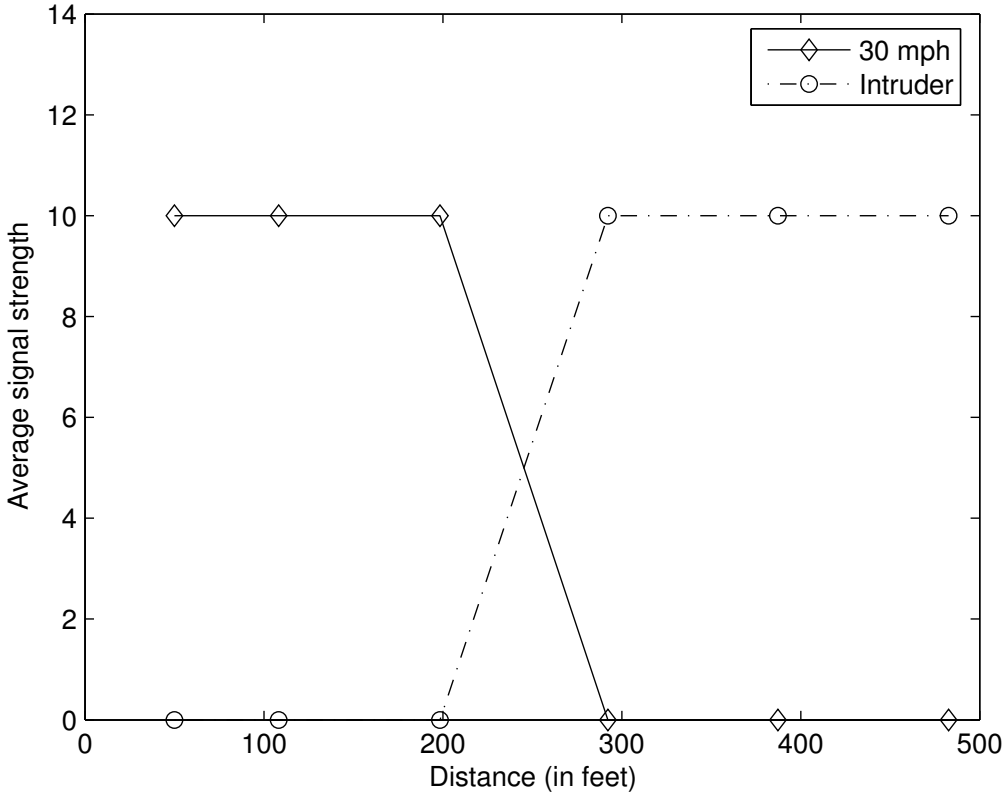

Fig. 43. Detection of intruder on foot while car driven at 30 mph on rough road

CHAPTER V

CONCLUSIONS

The sensitivity of the buried fiber optic intrusion sensor capable of detecting and locating intruders and moving vehicles has been investigated. The sensor is based on the principle of ϕ-OTDR, where the presence of an intruder is determined by the effect on the ϕ-OTDR trace of a phase change produced along the length of the fiber. An Er:fiber laser with a narrow linewidth and low frequency drift is used as the light source in the sensor system.

Field tests with different parameters affecting the performance of the sensor were performed. These tests were performed with the fiber buried in clay soil. The cable was buried at depths varying between 8 inches to 18 inches to study the sensitivity of the sensor to different burial depths. It was observed that in the regions where the fiber was buried shallower, the sensitivity was relatively higher than the other regions.

In the first series of tests, the sensitivity of the sensor to walking intruders of varying weights between 135 lbs to 195 lbs was characterized for three different buried cable test sections. It was observed that up to a distance of 5 ft to 7 ft from the sensor, an intruder could be sensed consistently with a high probability of detection. The probability of observing a "Very High" or "High" signal level varied from 73% to 100% and as expected, increased with the weight of the intruder. Shallower burial depths also generally yielded higher signal levels. The sensor could detect intruders even at a lateral range of 40 feet, where the average signal level was about 10% of the maximum average signal level observed when the intruder was directly over the buried cable.

In the second series of tests, a car was driven on a rough road with a closest

approach to the sensor of 50 ft and a smooth road with a closest approach to the sensor of 200 ft. The car was driven at varying speeds and the response of the sensor was studied. A car moving at 10 mph on a rough road could be detected up to a distance of 200 ft from the sensor. When the same car is driven at 30 mph it could be detected consistently on the trace up to a distance of 480 ft from the sensor. When the car was driven on a smooth road, its progress could not be observed on the trace unless it passed through a rough patch on the road.

The final series of tests were carried out to analyze the behavior of the sensor when an intruder and a moving car are simultaneously present. It was observed that when the car was driven at 10 mph the intruder could be distinguished when the car was about 108 ft from the sensor. When the speed of the car was increased to 30 mph, it was observed that the car had to travel farther away from the sensor ($\sim$200 ft) before the signal from the intruder could be sensed.

Based on these results we can conclude that the buried fiber optic sensor provides both high sensitivity and large dynamic range. Thus, it is a reliable surveillance and cueing system that alerts user to areas of likely activity or interest. The sensor also showed good sensitivity to both intruders and moving vehicles. The most surprising result is the ability of the sensor to detect intruders on foot at distances of 40 ft or more from the sensor line. Based on these results the sensor can be used in practical long range detection areas like national borders, nuclear facilities, chemical plants, electrical substations and military bases.

CHAPTER VI

RECOMMENDATIONS

Future work on the sensor should involve further investigations for improvement of the system performance for making it more reliable, accurate and as tamperproof as possible. Further field tests should be performed to study the relation between the sensitivity of the sensor to all the factors affecting it like burial depth of the fiber, type of soil and level of compaction of the soil. Since these sensors have different sensitivities when they are buried below different media, the sensitivities required for different types of media may be different. Therefore, the response of the sensor to different types of burial zones may also be characterized. The fading effect should also be studied in detail as it causes decrease in the probability of detection of an intruder.

The ability of the sensor to discriminate between different types of intruders should be explored. With suitable signal analysis and study of the characteristic signal from different intruders (like cars, animals, humans etc) it is possible that these intruders can be recognized. This will decrease the false alarm rates from environmental conditions (like underground utility lines) and animals. Another solution to reduce the false alarm rate due to animals is by mounting cameras at strategic locations and monitoring it to see what is moving at that location.

With further improvements the system can be calibrated for use on different types of buried zones, walls, fences and any place that has a barrier to prevent intruders from entering. In long remote stretches of border areas, parallel fibers along the main fiber can be provided for redundancy, false alarm reduction and tracking.

REFERENCES

[1] U.S Customs and Border Protection, "Border patrol," Available at: http://cbp.gov/xp/cgov/border_security/border_patrol, Sep. 2005.

[2] E. W. Maier, "Buried fiber optic intrusion sensor," M.S. thesis, Dept. of Elect. Eng., Texas A&M University, College Station, TX, 2004.

[3] K. N. Choi, J. C. Juarez, and H. F. Taylor, "Distributed fiber-optic pressure/seismic sensor for low cost monitoring of long perimeters," *Proc. SPIE*, vol. 5090, pp. 134–141, Apr. 2003.

[4] W. Seo, "Fiber optic intrusion sensor investigation," Ph.D. dissertation, Dept. of Elect. Eng., Texas A&M University, College Station, TX, 1994.

[5] K. N. Choi and H. F. Taylor, "Spectrally stable Er:fiber laser for application in phase-sensitive optical time-domain reflectometry," *IEEE Photon. Technol. Lett.*, vol. 15, pp. 386–389, Mar. 2003.

[6] J. M. Senior, "Optical fiber communications principles and practice," 2nd ed. New Delhi: Prentice Hall of India, 2001.

[7] J. C. Palais, "Fiber optic communications," 4th ed. New Delhi: Pearson Education Asia, 2002.

[8] Cisco Systems, "Fundamentals of DWDM technology," Available at: http://www.cisco.com/univercd/cc/td/doc/product/mels/cm1500/dwdm/dwdm_ovr.htm, Jun. 2004.

[9] J. Park, "Buried fiber optic sensor," M.S. thesis, Dept. of Elect. Eng., Texas A&M University, College Station, TX, 1992.

[10] S. V. Shatalin, V. N. Treschikov, and A. J. Rogers, "Interferometric optical time-domain reflectometry for distributed optical-fiber sensing," *Appl. Opt.*, vol. 37, pp. 5600–5604, 1998.

[11] B. Danielson, "Optical time domain reflectometer specifications and performance testing," *Appl. Opt.*, vol. 24, pp. 2313–2321, 1985.

[12] J. C. Juarez, "Distributed fiber optic intrusion sensor system for monitoring long perimeters," Ph.D. dissertation, Dept. of Elect. Eng., Texas A&M University, College Station, TX, 2005.

[13] J. C. Juarez, E. W. Maier, K. N. Choi, and H. F. Taylor, "Distributed fiber-optic intrusion sensor system," *J.Lightw Technol.*, vol. 23, no. 6, pp. 2081–2087, Jun. 2005.

[14] J. C. Juarez and H. F. Taylor, "Distributed fiber optic intruder sensor system for monitoring long perimeters," *Proc. SPIE*, Mar. 2005.

[15] S. A. Havstad, Y. Xie, A. B. Sahin, Z. Pan, A. E. Willner, and B. Fischer, "Delayed self-heterodyne interferometer measurements of narrow linewidth fiber lasers," *Conf. Lasers Electro-Optics (CLEO)*, pp. 310–311, May 2000.

APPENDIX A

EQUIPMENT USED

Electronic :

Oscilloscope: Tektronix 11201A Digitizing Oscilloscope

Pulse Generators: Tektronix PG501 and PG501 Pulse Generators

Function Generator: Hewlett Packard 3325B

Arbitrary Function Generator: Agilent 33220A

Current Source (for Pump Laser): ILX Lightwave LDX-3207B

DAQ Cards: National Instruments PCI-6111

Optical :

Optical Amplifier : Keopsys Fiber Amplifier KPSBTC13SDFA

Pump Laser: JDSU 29-8000-360-FL

Electro Optic Modulator (EOM1): JDSU 10023828

Electro Optic Modulator (EOM2): EOSpace SW-2x2-DOO-SFU-SFU

Photodetector: ThorLabs PDA400 Amplified InGaAs Detector

Fiber Spools: Corning SMF28

Couplers 50/50: AC Photonics WP15500102B2011

Couplers 90/10: AC Photonics WP15100102B2011

Isolators Dual Stage: AC Photonics IU15P21B11

Fiber Bragg Gratings (FBG) 1555.4 nm: Avensys (Bragg Photonics) Custom

Erbium Doped Fiber 18 dB/m: CorActive High-Tech Inc EDF-C 1400

Fiber Polarization Controller (for JDSU EOM): FPC030

Polarization Beam Splitter (PBS): Micro-Optics, Inc. PDM-IL-1550

Cable (Buried) 3 mm diameter (indoor)

VITA

Harini Kuppuswamy was born on December 7, 1980, in Chennai, India . She obtained her Bachelor of Engineering in electronics and telecommunication engineering from the University of Pune, India in May 2002. She worked as a research assistant in the Photonics Packaging Laboratory of the Chinese University of Hongkong, Hong Kong in the spring of 2003.

She joined the Electrical Engineering Department at Texas A&M University in August 2003. She graduated with a Master of Science degree in electrical engineering from Texas A&M University in December 2005. Her area of focus was optical engineering during her course of study at Texas A&M University. She can be reached at:

17W.704 Butterfield Road, Apartment #306,
Oakbrook Terrace, IL 60181.
Email: harini.kuppuswamy@gmail.com

The typist for this thesis was Harini Kuppuswamy.